A DISSERTATION ON
"ANALYSIS OF MULTIPARAMETRIC MRI DATA IN PROSTATIC CARCINOMA- PI-RADS AND CORRELATION WITH GLEASON SCORE IN A 3T MRI"

Submitted to

THE TAMIL NADU DR.M.G.R.MEDICAL UNIVERISTY CHENNAI

In Partial Fulfillment of the Regulations
For the Award of the degree

M.D. DEGREE BRANCH VIII
RADIODIAGNOSIS

MADRAS MEDICAL COLLEGE,
CHENNAI.

MAY -2018

CERTIFICATE

This is to certify that the dissertation titled **"ANALYSIS OF MULTIPARAMETRIC MRI DATA IN PROSTATIC CARCINOMA- PI-RADS AND CORRELATION WITH GLEASON SCORE IN A 3T MRI"** submitted by Dr.SAKTHIVEL RAJA.G , appearing for M.D.RADIODIAGNOSIS degree examination in April 2018, is a bonafide record of work done by him under my guidance and supervision in partial fulfillment of requirements of The Tamilnadu Dr. M.G.R Medical University, Chennai. I forward this to The Tamilnadu Dr. M.G.R Medical University, Chennai.

PROF. S.BABU PETER, MDRD
Guide,
Professor,
Barnard institute of Radiology,
Madras Medical College &
Rajiv Gandhi Government
General Hospital,
Chennai – 600 003.

PROF.R.RAVI, MD.,DMRD.,
Director & Professor,
Barnard institute of Radiology,
Madras Medical College &
Rajiv Gandhi Government
General Hospital,
Chennai – 600 003.

PROF.R.NARAYANA BABU, M.D., DCH,
Dean,
Madras Medical College &
Rajiv Gandhi Government General
Hospital, Chennai - 600 003.

DECLARATION

I, **Dr.SAKTHIVEL RAJA.G,** certainly declare that this dissertation titled, **"ANALYSIS OF MULTIPARAMETRIC MRI DATA IN PROSTATIC CARCINOMA- PI-RADS AND CORRELATION WITH GLEASON SCORE IN A 3T MRI"**, represent a genuine work of mine done at the Barnard Institute of Radiology, Madras Medical College and Government General Hospital, under the supervision of the **Prof. S. BABU PETER ,MDRD .,DNB.,** Barnard Institute of Radiology, Madras Medical College and Rajiv Gandhi Government General Hospital.

I, also affirm that this bonafide work or part of this work was not submitted by me or any others for any award, degree or diploma to any other university board, neither in India or abroad. This is submitted to The Tamil Nadu Dr.MGR Medical University, Chennai in partial fulfilment of the rules and regulation for the award of Master of Radiodiagnosis Branch VIII.

Dr.SAKTHIVEL RAJA.G

Date :
Place: Chennai

ACKNOWLEDGEMENT

I would like to express my deep sense of gratitude to the Dean, **Prof.Dr.R.NARAYANA BABU, M.D., DCH.,**Madras Medical College and **Prof.Dr.R.RAVI, MD.,DMRD.,** Director, Barnard Institute of radiology, MMC & RGGGH, for allowing me to undertake this study on **"ANALYSIS OF MULTIPARAMETRIC MRI DATA IN PROSTATIC CARCINOMA- PI-RADS AND CORRELATION WITH GLEASON SCORE IN A 3T MRI".**

I was able to carry out my study to my fullest satisfaction, thanks to guidance, encouragement, motivation and constant supervision extended to me, by my beloved Head of the Department **Prof.Dr.K.Malathi, M.D.R.D.,D.M.R.D.,** Hence my profuse thanks are due for her.

I would like to express my deep gratitude and respect to my guide **Professor Dr.S.Babu peter M.D.R.D.,D.N.B.,** whose advice and insight was invaluable to me. This work would not have been possible without her guidance, support and encouragement.

I am also extremely indepted to **Professor Dr.Kailasanathan M.D.R.D.,D.M.R.D.,our former director** for his valuable suggestions, personal attention, constructive cricticism during my study.My sincere thanks to **Professor Dr.S.Kalpana** for her practical comments and

guidance especially at the inception of the study and I also wish to thank **Prof.Dr.D.Ramesh** for his valuable support through out the study.

I am bound by ties of gratitude to my respected Associate Professors, **Dr.E.Manimekala, Dr.R.Ganga Devi** and **Dr.K.P.Kasi Visalakshi** and Assistant Professors, **Dr.Chezhian.J, Dr.Geetha.K, Dr.Geetha.G, Dr.Iyengaran.H, Dr.Mohideen Ashraf, Dr.Saranya.M, Dr.Balan.M.P, Dr.Dheebha, Dr.Karthik,** in general, for placing and guiding me on the right track from the very beginning of my career in Radiodiagnosis till this day.

I also thank **my past and present fellow postgraduates** who helped me in carrying out my work and preparing this dissertation. I thank **all the Radiology technicians, Staff Nurses and all the Paramedical staff members** in Barnard Institute of Radiology, for their fullest co-operation. I thank my statistician **Mr.Venkatesan**, who rendered his valuable timely help in completing this study.

I thank my **lovable parents and my sisters** for their constant and persistent support for my studies and in all my endeavours. My heartfelt thanks to **my wife**, for her endless support, continued and unfailing love, which helped me to overcome the difficulties encountered in the pursuit of this degree.

I would be failing in my duty if I don’t place on record my sincere thanks to those **patients and their relatives** who inspite of their sufferings extended their fullest co-operation to the study.

Dr.SAKTHIVEL RAJA.G

TABLE OF CONTENTS

SL.NO	CONTENTS	PAGE
1	INTRODUCTION	1
2	AIM AND OBJECTIVES OF THE STUDY	5
3	REVIEW OF LITERATURE	6
4	MATERIALS AND METHODS	45
5	STATISTICAL ANALYSIS	52
6	OBSERVATON AND RESULTS	54
7	DISCUSSION	61
8	LIMITATIONS OF THE STUDY	73
9	CASES	74
10	CONCLUSION	80
11	BIBLIOGRAPHY	
12	ABBREVIATIONS	
13	ANNEXURES Patient proforma Patient information sheet Patient consent form Master chart Ethical committee approval Digital receipt of plagiarism Plagiarism	

INTRODUCTION

Carcinoma of prostate is one of the leading causes of cancer death among aged men. It is the most common non-cutaneous cancer among men [(1)]. The incidence of prostate cancer is on the rise primarily because of increased application of screening tests using prostate-specific antigen (PSA) and also partly because of the increase in life expectancy [(2)].

Most of the prostate cancers are slow-growing and indolent rather than being aggressive and hence they seldom produce any symptoms until the advanced stage. Hence, early diagnosis of prostate cancer can lead to improved treatment outcomes besides aiding in the selection of multiple treatment options available.

Traditionally, the methods employed include a prostate-specific antigen assay (PSA), Digital rectal examination (DRE) and Transrectal ultrasound guided biopsy (TRUS). The confirmatory diagnosis of prostate cancer can only be made by taking a biopsy which is usually a 8-core TRUS biopsy. However, all these methods have their own limitations and disadvantages.

PSA assay levels lack sensitivity and specificity while the DRE is a crude technique with a low positive predictive value and high inter-observer variability. Studies have shown that TRUS biopsy can miss

upto 20% of prostate cancers because of under sampling of anterior prostate, apex and midline resulting in high false negativity [3].

About 70% of initial biopsies performed in men with raised PSA levels are negative for prostate cancer hence increasing the burden of negative biopsies and increased screening costs [4].

Because of these limitations of the currently existing techniques, the search for a diagnostic technique which is reliable, sensitive, specific with good positive and negative predictive values besides being non-invasive have led the researchers to consider radiologic imaging techniques like magnetic resonance imaging (MRI) as a diagnostic tool and especially multi-parametric MRI (MP-MRI) has received quite an attention in the recent years which builds upon the regular advantages of MRI.

Multi-parametric MRI (MP-MRI) combines the anatomical imaging in T1 and T2 weighted images with the 2 functional methods like diffusion-weighted imaging (DWI), dynamic contrast enhanced imaging (DCE) with or without Magnetic resonance spectroscopy (MR spectroscopy).

MP-MRI aids in pre-biopsy diagnosis of cancer prostate, provides guidamce for biopsy- either real-time or cognitive TRUS guided biopsy or fusion biopsy.

It also helps in characterizing the extent of the disease involvement which can aid in minimally-invasive procedures. Moreover it also helps in predicting the treatment outcomes and selecting amongst the various treatment options available.

Furthermore, diffusion-weighted imaging (DWI), dynamic contrast enhanced imaging (DCE) and Magnetic resonance spectroscopy shows promise in better characterization of the lesions and assessment of cancer aggressiveness in correlation with low, intermediate and high Gleason scores. Gleason‘s grading system is the standard histo-pathological method for estimating aggressiveness of prostate cancer[6,7].

It is used to describe a tumor as low grade (Gleason‘s score ≤6), intermediate grade (Gleason‘s score = 7), or high grade (Gleason‘s score >7) with respect to tumor aggressiveness. The probability of disease recurrence increases with increasing Gleason‘s score and increasing percentage core involvement of tumor in biopsy specimens[8,9]. Hence, accurate scoring is necessary to determinate appropriate therapy, according to risk groups. Active surveillance for low risk tumors (Gleason‘s score ≤6), monotherapy for intermediate risk tumors (Gleason‘s score = 7) and combination therapy for high risk tumors (Gleason‘s score, >7) are the best treatment options.

Even today, the confirmatory diagnosis of prostate cancer lies in the histologic examination performed on a biopsy specimen and application of Gleason scoring for grading of the two most common patterns of the cells from 1 (lowest) to 5 (highest) and adding them to yield a score with a maximum of 10 and scores above 7 are considered adverse towards prostate cancer.

This study was planned to assess the efficacy of multi-parametric MRI in detection of prostate cancer in correlation with Gleason scores of the biopsies among the men with raised prostate-specific antigen (PSA) levels.

AIM AND OBJECTIVES

AIM

- To evaluate the efficacy of **Multiparametric MRI as a noninvasive investigation in detection of carcinoma prostate** in patients with raised PSA level and to correlate PI-RADS values with Gleason‘s score of prostate cancer.

Objectives

- To determine the relationship and correlate apparent diffusion coefficient (ADC) values with Gleason‘s score of prostate cancer.
- To determine mean ADC values for low risk (Gleason‘s score <6), intermediate risk (Gleason‘s score = 7) and high risk (Gleason‘s score >7) prostate cancer.

REVIEW OF LITERATURE

According to American cancer society (ACS), screening for prostate cancer should be annual and should include high risk men with age above 50 years and with life expectancy of at least 10 years and in men with strong family history of prostate cancer in the first or second degrees relatives.

There are multiple modalities of treatment available for prostate cancer depending upon the stage of the disease. Early diagnosis by applying screening methods has shown to improve the treatment outcomes.

Currently, screening is based on elevated prostate-specific antigen assay (PSA) levels and an abnormal Digital rectal examination (DRE) revealing a nodule which prompts the physician towards a Trans-rectal ultrasound guided biopsy (TRUS) of prostate which leads to a confirmatory diagnosis of cancer usually using a 8-core TRUS biopsy. This 8-core TRUS biopsy is not fool-proof in that it leads to many false negative biopsies as it does not sample the exact location of tissue suspected of malignancy and also in many cases there are high number of negative biopsies.

Furthermore, diagnosing men with raised PSA levels is critical as they run a significant risk of malignancy. Also, there is much higher

rates of overlap between benign prostatic hyperplasia (BPH) and prostate cancer in patients with raised PSA levels. The absence of exact cutoff for PSA levels to recommend the TRUS biopsy necessitates an improved screening tool with better accuracy, sensitivity, specificity and predictive value. Moreover TRUS biopsy is an invasive procedure causing much discomfort to the patient given its high false negative results.

Magnetic Resonance Imaging [MRI] is known for its potential to produce high resolution anatomical images non-invasively. With a lot of research to improve its diagnostic capability, additional imaging features like functional imaging, metabolic imaging and diffusion imaging etc. with faster image generation and high image resolution emerged in the last decade and has shown much promise in many a fields.

Prostatic MRI with T1 and T2 weighted imaging was used in 1980s but it lacked sensitivity and specificity. Also Magnetic Resonance Spectroscopy (MR spectroscopy) has shown its way in improving the diagnostic potential of the regular conventional MRI. Another advantage is that MR spectroscopy demands only an additional software upgrades along with a regular MRI machine which adds a little bit for the cost factor.

The combined use of all these techniques along with conventional anatomical imaging has shown to increase the sensitivity and specificity of MR imaging in diagnosing prostate cancer especially when diagnosis is doubtful in men with raised PSA levels[9].

Multi-parametric MRI (MP-MRI) has gained much attention in the recent years both as a screening and diagnostic tool for prostate cancer and also it has shown to clearly delineate anatomical defects in prostate gland(10).

Multi-parametric MRI (MP-MRI) consists of anatomical and functional MR techniques such as T1 and T2 weighted MRI, diffusion weighted MRI imaging (DWI), dynamic contrast enhanced – MRI (DCE-MRI) and MR spectroscopic imaging (MRSI).

T1 weighted imaging detects bleeding spots within the prostate gland which is very common after previous biopsies while T2 weighted imaging depicts the zonal anatomy of the prostate with precision[11]. The downside of the T2 weighted imaging is that even benign prostatic hyperplasia can produce low signal intensity depending on the stromal component of the gland. This affects the diagnostic potential regarding carcinoma in the transition zone.

Moreover, benign conditions like prostatitis, hemorrhages in the gland, changes and fibrosis due to radiation therapy and hormone

deprivation therapy can also produce hypo intense images in T2 weighted imaging in the peripheral zone.

Diffusion-weighted MRI (DW-MRI) estimates the diffusion of water through the cellular level of the gland and decreased free diffusivity indicates prostate cancer due to the increased cellularity in the gland [11].

The reduction in free diffusivity of water can be estimated quantitatively using apparent diffusion coefficient (ADC) maps. The levels of ADC maps correlates negative linearly with Gleason scores in prostatic carcinoma [12].

Dynamic contrast enhanced MRI (DCE) gives information regarding the tumour angiogenesis and is a non-invasive technique. In comparison to normal prostate gland, DCE images in prostate cancers show steep wash-in slope, high peak enhancement and rapid wash-out [11]. But the disadvantage is lack of its specificity and sometimes, prostatitis in peripheral zone and BPH nodules in the central zone can produce earlier and more enhancement than the normal prostatic tissue [13] .

Currently MRI is the only imaging modality with very good spatial resolution and soft tissue contrast necessary to clearly depict the localized prostatic cancer. Recently the availability of 3 Tesla magnets has reduced the acquisition time greatly and also provides

superior anatomical definition and details in comparison to the previously used 1.5 Tesla magnets [14].

Moreover the previous 1.5 Tesla magnets used endorectal coils but they are not necessary for the currently used 3 Tesla Magnets, thus greatly reducing the cost, time and also patient discomfort [15]. A review by a recent study group has revealed that mp-MRI reliably detects prostatic cancer which are clinically significant and also produces the exact tumor location and staging besides the tumor volume and also the grade of the tumor [14].

The following table clearly depicts the components of MP-MRI and its individual advantages, disadvantages:

Table 1: Components of Multi-parametric MRI (14)

Components of Multi-parametric MRI	**Description**
T1-weighted Imaging	Differentiates between tumour and post-biopsy haemorrhage.
T2-weighted Imaging	Clearly defines prostate anatomy by high resolution images Due to high water content the normal peripheral zone is shows intermediate to high signal intensity Cancer shows low intensity because of increased cellularity

Components of Multi-parametric MRI	Description
	Best way to assess the extracapsular extension outside the prostate margins, seminal vesical invasion, adjacent organ spread and involvement of neuro-vascular bundle. Lacks accuracy in the anterior zones and transitional zones as the baseline signals is lower and BPH nodules are very common here. When used alone, T2WI does not have the sensitivity and specificity enough for the localisation of the prostatic cancer and hence it is not used for functional imaging.
Diffusion weighted imaging (DWI)	Measures the free diffusion of water through the tissue Because of increased cellularity and tightly packed cells in carcinoma of prostate, there is reduced diffusion of water. The apparent diffusion coefficient maps (ADC) are derived and interpreted along with T2WI. When both these are combined the sensitivity and specificity of DWI and T2WI is about 85 to 90% in comparison to radical prostatectomy findings.
Dynamic contrast enhanced imaging (DCE)	Bolus of IV gadolinium is a given and a T1 sequence is run followed by a rapid sequence of scans. Increased blood flow, neo-vascularity and leaky capillaries are signs of malignant tissue. Perfusion to the pre-determined area can be plotted against time to create a perfusion vs time curve and can

Components of Multi-parametric MRI	Description
	be analysed. There can be 3 types of curve like Type 1 : Normal prostate tissue Type 2 : BPH & prostatitis Type 3 : High grade prostate cancer 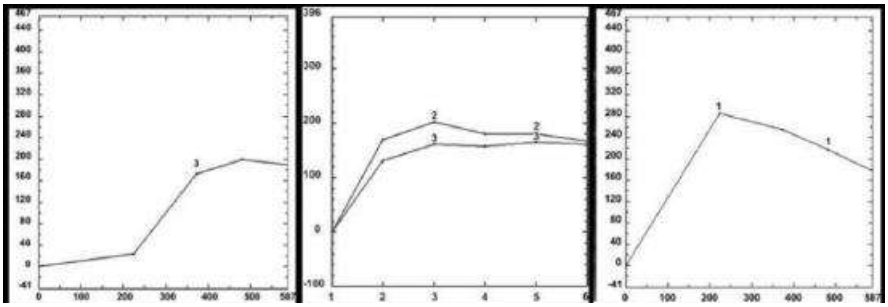 Type 1(Persistent Increase) Type 2 (Plateau) Type 3 (decline after initial upslope)
Magnetic resonance spectroscopy (MRS)	Indirectly measures the metabolite levels in the prostatic tissue and hence it is largely a functional technique. Cellular concentration of choline and creatine increased in prostatic cancer and their levels correlate with the volume and grade of the tumour. The technique is technically challenging and also time consuming and sometimes it is not included in the mp-MRI sequence.

DIFFUSION WEIGHTED IMAGING

Diffusion weighted imaging (DWI) is another MR based technique that probes the functional characteristics of tissues. It was introduced by Stejskal and Tanner in the early-1980s[16-18]. In conventional MR imaging, diffusion of water molecules in the tissues provides an extremely small contribution to MR signals. In DWI, powerful magnetic gradients are used to detect thermally driven water molecules. Molecular diffusion in tissues is not free, but reflects interactions with many obstacles, such as macromolecules, fibers and membranes. Rate of diffusion of water molecules is determined by cell density, membrane, intracellular elements and macromolecules. Therefore, the rate of diffusion of water molecule can reveal microscopic details about tissue architecture either in a normal or diseased state. In diffusion weighted imaging (DWI), the intensity of each image element (voxel) reflects the rate of diffusion of water molecules at that location.

Diffusion weighted imaging was initially used in neuroimaging in 1985[19]. DWI is more sensitive when the tissue of interest is dominated by isotropic water movement[20]. e.g., gray matter in the cerebral cortex and major brain nuclei or in the body—where the diffusion rate appears to be the same when measured along any axis. It was used in the study and treatment of neurological disorders, especially for the management of patients with acute stroke. Gradually, its role has been extended to

characterize abdominal and pelvic lesions [21,22]. One of the most promising application among them is the detection of prostate cancer with DWI.

However, DWI also remains sensitive to TI and T2 relaxation. To entangle diffusion and relaxation effects on image contrast, one may obtain quantitative images of the diffusion coefficient, or more exactly the Apparent Diffusion Coefficient (ADC) maps.

Conventionally, three gradient directions are used in diffusion weighted imaging, which are sufficient to estimate the trace of the diffusion tensor or 'average diffusivity'.

To sensitize MRI images to diffusion, the homogeneous magnetic field is varied linearly by a pulsed field gradient. Since precession is proportional to the magnet strength, the protons begin to precess at different rates, resulting in phase dispersion and signal loss.

Another gradient pulse is applied in the same magnitude, but with opposite direction to refocus or rephase the spins.

The refocusing will not be perfect for protons that have moved during the time interval between the pulses, and the signal measured by the MRI machine is reduced.

APPARENT DIFFUSION COEFFICIENT

Apparent diffusion coefficient is the quantitative measurement of the diffusion, which measures the average area, covered by a molecule per unit time and is measured in millimetre square per second.

CALCULATION OF ADC VALUE

Calculation of ADC value is based on the attenuation in signal intensity between at least two diffusion-weighted images according to the following equation:

$$ADC = (1/ b1 - b0) \ln (S[b1]/S[b0])$$

Where b1 and b0 represents two different b values, S[b1] signal intensity of the selected ROI on the slice level acquired with b-value b1, and S[b0] signal intensity of the same ROI on the same slice level acquired with b-value b0.

Tissues with restricted proton diffusion have low ADC values as seen in the malignant tumors. In the body, ADC measurement includes factors such as diffusion and perfusion, therefore the term apparent diffusion coefficient is used:

$$\text{ADC value} \approx D + (f/b)$$

Where D = diffusion coefficient and f = perfusion factor. The effect of perfusion can be decreased by using higher b values.

FACTORS AFFECTING ADC VALUES

Various factors such as cellular density, cell membrane permeability, viscosity of the fluid and microstructure of the biological tissues can affect the ADC value. An ADC map is a software generated image which can be a colour scale or gray scale image representing the intravoxel ADC values. On clinical MRI scanners, diffusion sensitivity is easily varied by modifying the parameter known as b value, which is mainly proportional to the gradient amplitude and duration.

The images acquired with low b values are less diffusion weighted because they use less gradient. On the other hand, the high b value images are strongly diffusion weighted but have lower signal-to-noise ratio (SNR). The diffusion sensitivity is also affected by perfusion when low b values are used which spuriously results in higher ADC values[23]

DWI is typically performed using at least two b values to enable a meaningful interpretation. In theory, the error in ADC calculation can be reduced by using multiple b values. However, the scan duration will be prolonged with increasing number of b values. Moreover, there is no consensus as to how many and which b values should be used to differentiate benign and malignant lesions.

DWI has been shown to improve the detection of prostatic cancer with varied sensitivity and specificity[24-28]. b value upto 1000 s/mm^2 are commonly used to detect prostate cancer. However there is no

appropriate consensus on optimal b value to be used for detection of prostate cancer. Higher b values may increase the accuracy of cancer detection in transitional zone but lowers signal-noise ratio [29,30].

Several recent studies have proven the potential of DWI to differentiate benign and malignant prostate lesions based on low ADC value in malignant lesions. These studies used different b values, varying from 0 to 1,000 s/mm2, and found a significant difference between the ADC values of malignant and benign lesions [31-35].

CITRATE METABOLISM IN PROSTATE

The citrate molecules synthesized during this process via the TCA cycle is the source for acetyl-coA which is required for the lipogenesis. The Krebs cycle and the other recycling process of the intermediate molecules are very much indispensable for the metabolism of the amino acids.

On the other hand, the normal prostatic tissue does not go through this process of citrate oxidation and thus usually large amounts of citrate accumulates in the gland as a product of intermediary metabolism.

Cooper and Imfeld et al reported for the first time that the normal levels of citrate in the prostatic tissue is decreased in cases of prostatic cancer and not in normal tissue or in cases of BPH[36].

After some research this same group indicated that these biochemical alterations at the cellular levels may occur well in advance in cases of cancer even before the appearance of histologic changes[37].

It was during the last decade that many research surfaced regarding the measurement of citrate levels in the prostate as a diagnostic tool for early diagnosis of cancer.

Costello, Franklin et al shed some light in the involvement of zinc in the production of citrate inside the tissue after analysing the biochemical alterations at a cellular level[38,39] .

Usually in the central zone of prostate, the levels of zinc and citrate are at a very low concentration[40]. Because of the presence of zinc in this zone, the mitochondrial aconitase activity which is involved in the oxidation of citrate is very much limited in the normal epithelial cells. Accumulation of citrate is at the expense of ATP production which is reduced to about 65% in the normal prostate epithelial cells (14 moles of ATP) compared to the other mammalian cells which completely oxidizes the glucose molecule (38 moles of ATP).

However in case of prostate cancer, the ability for the intra-mitochondrial accumulation of zinc in cancer cells is diminished. This major change in zinc concentration leads to restoration of the – aconitase enzyme activity and hence leads to increased citrate

oxidation. This oxidation of citrate coupled with ATP production is essential step towards the progression of malignancy [39, 41, 42].

Although many interactions between zinc and citrate are being under the scanner in recent years, there are evidences suggesting that they play a significant role in pathogenesis of prostatic carcinoma.

MAGNETIC RESONANCE IMAGING

Many recent studies show that combined use of phased array coil and endorectal along with the high field strength magnets can provide high image resolution [43].

More recently the new 3.0 Tesla magnets used in the upgraded MRI systems have obviated the use of these endorectal coils and hence it has contributed for reduction of cost and also very importantly time and discomfort of the patients who are usually aged persons.

MR imaging has always been the method of choice for accurate depiction of the internal prostatic anatomy with clear delineation of the zones. It also displays the complex physiology of the gland.

Over the past decade, the superiority of MR imaging in the staging and grading of prostatic malignancy especially involving the peripheral zone has been reported to be between 75% and 90% consistently [44].

Most of the prostatic cancers usually involves the peripheral zone of the gland where the malignant tissue is identified as one which shows a low signal abnormality in T2 weighted imaging.

Though MRI has allowed for intra-prostatic evaluation of tumour location, the results for diagnosing the exact extent is non-specific [45].

Torricelli et al observed that carcinoma in this regions can mimic post-biopsy haemorrhage, scar, inflammation or intra-glandular dysplasia on MRI imaging using T1 and T2 anatomical imaging with a very low specificity of just 50%. [26]

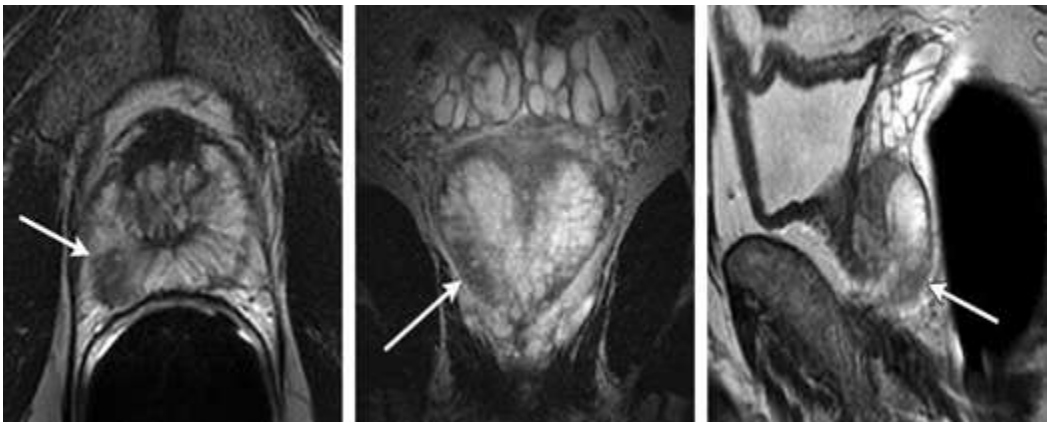

Figure 1. Malignant foci in the peripheral zone of prostate gland

MAGNETIC RESONANCE SPECTROSCOPY (MRSI)

It is a powerful tool which can provide biological information regarding the many metabolites involved in the prostatic physiology and carcinogenesis[47]

The Proton spectroscopy is very promising in terms of spatial resolution, sensitivity, , signal to noise and acquisition time. This

technique has been commonly used for imaging in the brain and its application for other anatomical regions is also expanding at an enormous rate.

MRSI provides the chemical makeup of the images area and hence helps in determining the physiological abnormalities of the imaged region in comparison to the normal tissue. This technique can indirectly assess the carcinogenic changes in the metabolite levels and molecules studied in MRSI includes water, choline, lipids, citrate, creatine, lactate and aminoacids[47].

As previously stated, the prostate gland is very unique in the body because of the fact that it contains high citrate levels[48] .When the normal prostatic glandular epithelial cells get replaced by the neoplastic cells the citrate concentrations and choline change in the transformation to a malignant state. In the presence of active malignancy, typically choline levels increase and citrate levels tend to fall [49].

The genesis behind the reduced concentrations of citrate has been discussed before but the reason behind the increased concentration of choline levels is much less understood as in case of brain spectroscopy.

The hypothesis behind this is that choline elevation is associated with changes in the synthesis and degradation of cell membrane which is very common in cases of malignancy.

The choline resonance observed in-vivo at 3.22 ppm is sometimes referred to as total choline.It arises from methyl hydrogens of trimethylamines and consists of choline, glycerophosphocholine (GPC), phosphocholine (PC), glycerophosphoethanolamine (GPE), ethanolamine and phosphoethanolamine (PE) [50 - 54] .

These compounds are indispensable for the synthesis and hydrolysis of phosphatidylcholine and phosphatidylethanolamines which form the integral part of the bilayer structure of the cells and regulate the membrane function and stability.

Polyamines like spermine can be visualized in the prostatic MRSI [51]**.** These molecules are involved in many cellular processes such as maintenance of DNA structure, RNA processing, Protein activation and translation[56, 57]**.**

Any change in the polyamine molecules has been shown to influence the modulation in the genetic effects of the genes. It is visualized as a broad peak between choline and citrate in the proton MRSI.

In contrast to the normal epithelial cells which demonstrate high levels of citrate and polyamines like spermine, the cancerous tissue shows a decline in levels of these crucial metabolites and to the extent

that the creatine resonances and choline are resolved even in the baseline.

The unfortunate limitation of MRSI is that because of the necessity for suppressing lipids to minimize the contamination from lipids surrounding the prostate gland, monitoring of metabolites such as lipids and lactate in vivo is affected.

In-vitro studies have shown that citrate to lactate ratio can be used to differentiate prostatic malignancy and BPH. This ratio can be used to study the aggressiveness of the cancer tissue[37.]

MRSI TECHNIQUES

The MRSI of the brain is the most developed technology. The translation of this technique to other body parts including prostate gland has not made giant steps instead it has been trivial in the last decade.

The possible movement of prostate gland during the acquisition of MRI sequences besides the dominating triglyceride signals from the adipose tissue surrounding the prostate gland has become a great challenge to MRSI in providing reliable and quality spectral data.

Studies in prostate spectroscopy used Point resolved spectroscopy (PRESS) and single voxel techniques such as STEAM (Stimulated echo acquisition method) using the body coil [58 - 61].

Usually in these cases the voxel size was large enough and encompassed both the central part of the gland and also the peripheral zone. The limitation of these techniques are poor signal to noise of the spectra and long scan times. This greatly reduced its application in the clinical setting although it showed the feasibility of performing the proton spectroscopy.

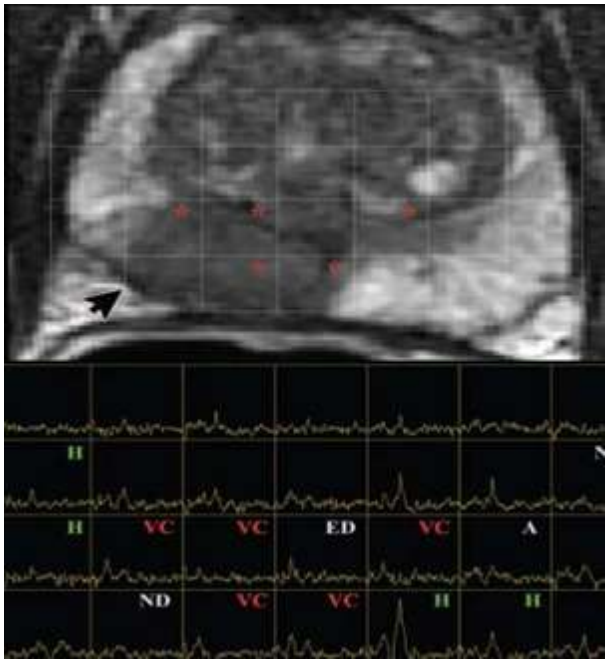

Figure 2.MRSI with voxels

The interest in spectroscopy of prostate increased manifold largely after the introduction of 2D and 3D MRSI technologies [62-65].

There was a need of technology to reliably detect the resonances from the relevant biological compounds in the gland and to accurately localize the signals, which can suppress the large signals from both water and lipids from the surrounding areas. This was rightly addressed by the 3D spectroscopic MRSI techniques[66 - 69].

The advantage of the 3D-MRSI technique is that it has the ability to provide the data with high spatial resolution. It also provide the best prostate metabolite information for the entire gland.

The convention is that to use Band selective excitation with gradient de-phasing (BASING) and PRESS localization for lipid and water suppression[66].

The 3D-MRSI by using the contiguous voxels can produce an array of spectra depicting the entire prostate gland and these contiguous spectral array with mapping of the entire gland coincides with the T1 and T2 weighted images allowing for the comparison and interpretation between the anatomical images besides the metabolic information.

Studies showed that 3D-MRSI can be used in an additional setting to differentiate the tumor foci with near-perfect localization of the tumor to the volume size as small as 0.24cc [70 - 74].

Nijmegen et al further refined the 3D-MRSI technique by using the elliptical encoding and reduced the scan times even further [75-77].

The combined evaluation of the prostate gland by using both MR images and MRSI leads to the most confident identification of cancer prostate with increased specificity of upto 98%[75]

The results like low signal intensity in T2 weighted imaging along with decreasing levels of citrate and also polyamines along with a

concomitant rise in the levels of choline increases the specificity of this combined evaluation of prostate gland in diagnosing the malignancy to many a fold. Therefore an increased choline to citrate ratio is usually suggestive of prostatic malignancy. Many researchers use (choline + creatine) / citrate ratio for spectral analysis as the choline and creatine resonances are inseparable for quantification.

The 3D-MRSI provides volumes of spectroscopic data and a standardized scale necessary to make the task of spectral analysis.

It is easy for the radiologists and physicians and also such standardized scales will help in characterizing the tumor aggressiveness besides the exact spatial extent of the tumour[78.] The combination of MRSI and MRI along with other functional techniques is emerging as a sensitive tool for metabolic evaluation and anatomic details of the prostate gland [79, 80]

Recent research in MR technology and pulse sequences has led to acquisition of metabolic information from the entire prostate at high resolution and also within a reasonable time of less than ten minutes.

Proton MRI/MRSI is of great value in patients with increased risk of cancer like the men with elevated PSA levels between 4 and 10 ng/ml and also for patients on active surveillance on longitudinal

follow-up from the therapy and also in guiding localized treatment techniques[81 - 83]

MRSI techniques have largely benefitted from the newer generation of ultra-high field magnet systems and also because of the emergence of multi-channel parallel imaging [84 - 86].

IMAGING OF PROSTATE

TRUS of the prostate was first described by Wantanabe et al [87] and this TRUS expanded to routine clinical use with simultaneous improvements in ultrasonography and the significant step in the history of TRUS was made when Hodge et al [88, 89] used and demonstrated a TRUS-guided systematic sextant biopsy protocol.

Concomitantly with the increased use of PSA assay as a screening method for prostate cancer, the number of men who underwent TRUS guided biopsy increased greatly to as high as an estimated 800,000 biopsies in the United States alone annually [90]

Because of the sheer patient load for the TRUS-guided biopsy and given the ever-rising prevalence of prostate cancer, the need for appropriate protocol for biopsy indications and the ideal technique to image and biopsy the prostate also was also very high.

Even today in many parts of the world, TRUS technology has been used as the mainstay of many image guided prostatic interventions

such as prostate needle biopsy, brachytherapy, cryotherapy and also high intensity focused ultrasound (HIFU).

TRUS has shown its application and use in the appropriate evaluation of patients with benign prostatic hyperplasia [91].

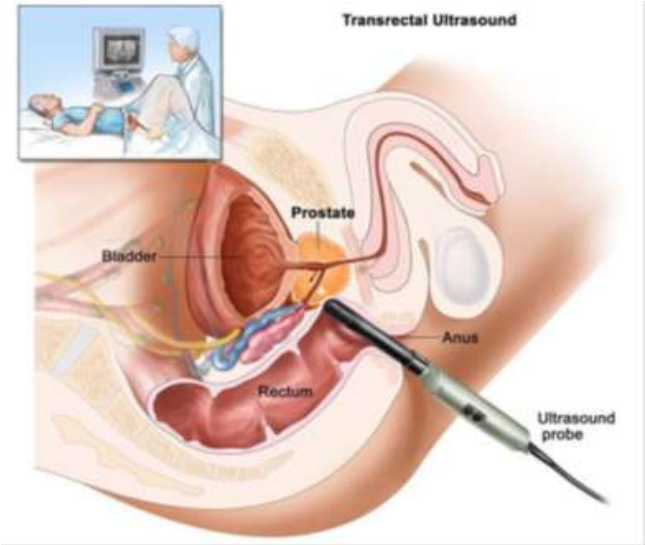

Figure 3. Normal appearance of prostate in TRUS

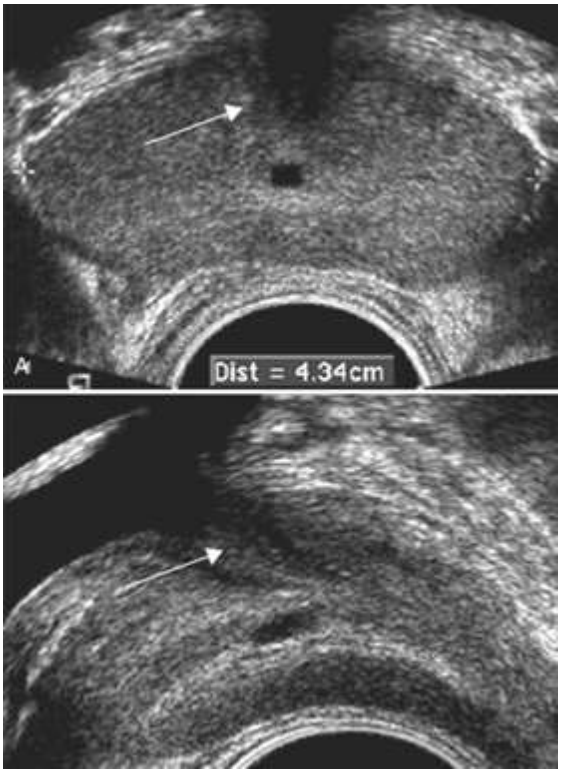

ULTRASONOGRAPHIC ANATOMY OF THE PROSTATE

The prostate gland lies between the bladder neck and the urogenital diaphragm and is just anterior to rectum which is used as an ideal position for imaging via TRUS. Traditionally the prostate gland has been described based on the pathologic zonal architecture. This consists of an anterior fibromuscular stroma (AFS) that is completely devoid of glandular tissue, transition zone (TZ), central zone (CZ), peri-urethral zone and peripheral zone (PZ). But unfortunately these demarcations into zones cannot be made clearly on sonography.

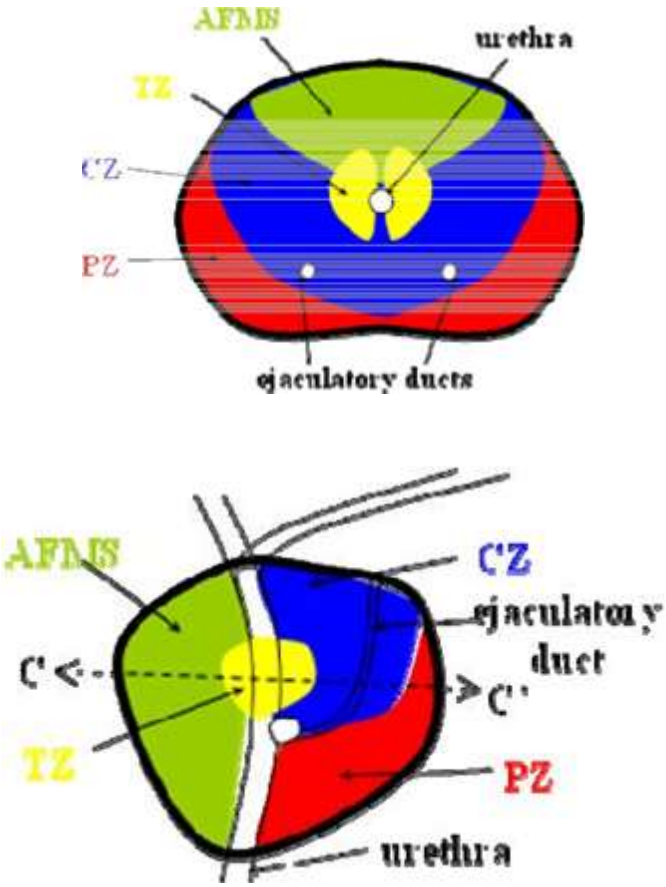

Figure4. Prostate anatomy

But sometimes especially in cases of Benign prostatic hyperplasia (BPH), the transition zone (TZ) can be discernible from the peripheral and the central zone. The normal CZ and PZ is located posteriorly and is considered the seat for majority of the adeno-carcinomas and they have a very homogeneous echogenic appearance in imaging while the anteriorly located transition zone gives varied heterogeneous signals.

PROSTATE CANCER IMAGING IN TRUS

All hypoechoic lesions within the peripheral zone should be noted and be included in the biopsy material. The lack of very distinct hypoechoic foci does not preclude proceeding towards biopsy because of the fact that 39% of all the cancers are iso-echoic and up to 1% of cancers may be hyperechoic on conventional TRUS [92].

In spite of the high prevalence of prostate cancer among the hypoechoic areas in the peripheral zone, the presence of hypoechoic areas itself is not associated with increase in cancer rates compared with the biopsy cores from isoechoic locations in a contemporary series of almost 4000 patients [93].

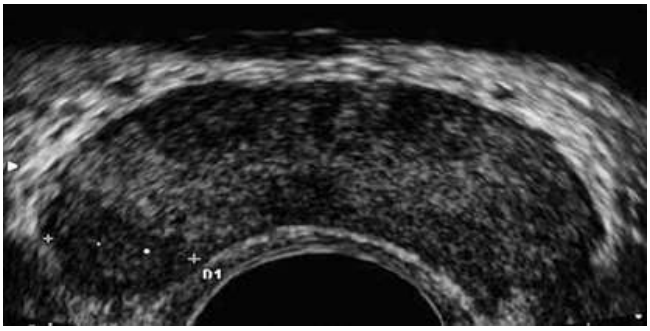

Figure 5. TRUS image in prostatic carcinoma

COLOR DOPPLER AND POWER DOPPLER TRUS

It is based on the shift of the frequency of the reflected sound waves from the frequency of insonation and hence it depicts the velocity of blood flow in a direction dependent manner.

Assignment of color is based on the direction of blood flow which is related to the orientation of the transducer which is receiving the signal and also the flow towards the transducer is depicted a red color while the flow away from the transducer is depicts a blue color. The color is not specific for arterial or venous blood flow.

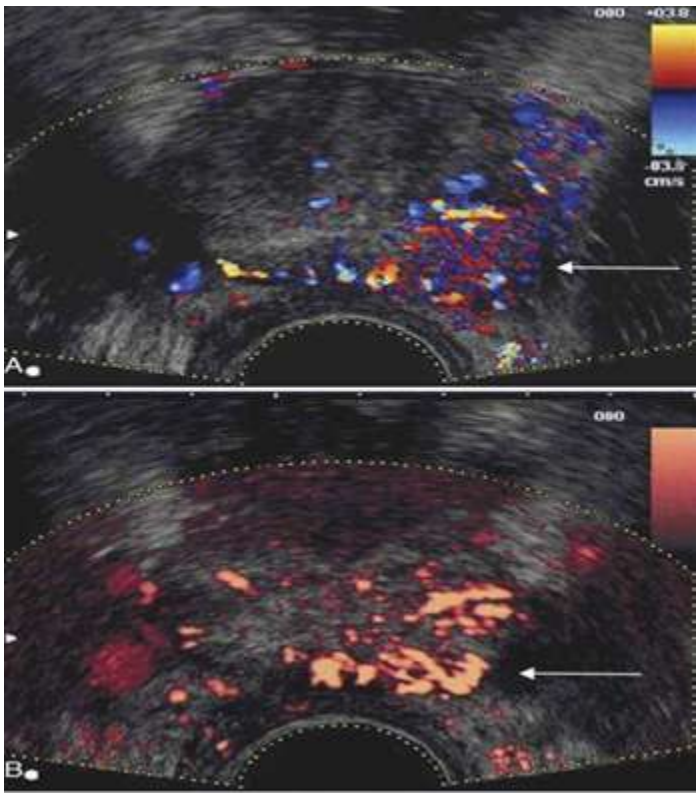

Figure6. TRUS with color and power Doppler

Power Doppler utilizes an amplitude shift to detect the flow velocity and in a directionally independent manner [94]. The major

advantage of the power Doppler is that it has the ability to detect even the slow flow rate.

It also has lesser reliance on the Doppler angle which makes this technique suitable for detection of neo-angiogenesis in cases of prostatic malignancy and hence has high sensitivity in detecting the slower flow rate.

Although the power Doppler technique has this distinct advantage over the color Doppler, neither of these 2 techniques has proven it's superiority in the diagnosis of prostate cancer. Enhancement of the color Doppler TRUS using the contrast agents provides the necessary push to identify the extent of cancer localization within the prostate.

Of late sonography has evolved generating a new technique called elastography which is considered by some as superior to color Doppler imaging in identification of prostate cancer [95-96].

Elastography technique uses the real-time sonographic imaging of the prostate at baseline level and also under varying degrees of compression. Through appropriate computer software and calculations, differences in displacement of ultrasonic images can be studied from baseline and in comparison to images taken during compression and hence regions with decreased tissue elasticity may be tagged as suggestive areas of malignancy.

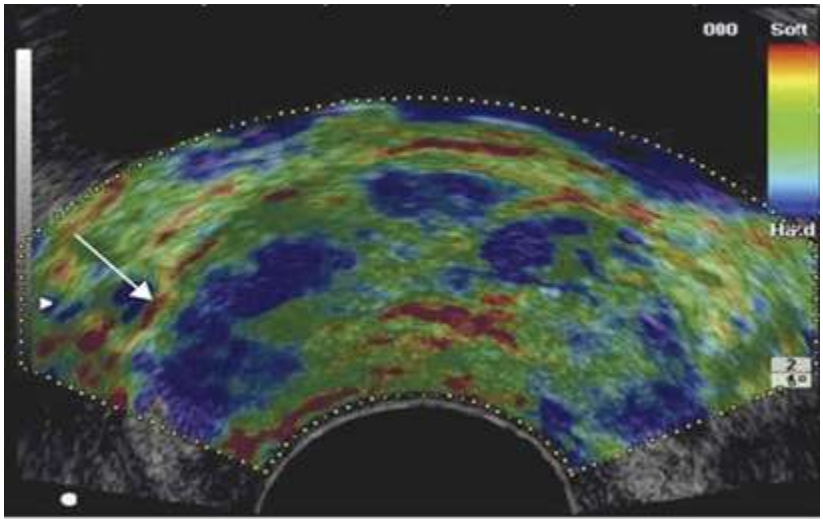

Figure 7. Elastography of prostatic malignancy

A variety of imaging modalities have been studied in diagnosing and staging the extent of prostate cancer but unfortunately even today not a single technique has promised to displace systemic TRUS gray-scale core needle biopsy as the gold standard for the diagnosis of prostatic malignancy except multi-parametric MRI although it has its own limitations.

The inability to diagnose microscopic disease limits the accuracy of almost all the imaging modalities.

But this limitation has been partly overcome by the use of multi-parametric MRI as it combines multi-modal imaging functions like metabolic imaging, functional imaging and anatomical imaging.

There are innumerable research studies showing the advantages and disadvantages of the individual components of multi-parametric

MRI but studies comparing the efficacy of multi-parametric MRI on the diagnostic front in comparison to Gleason scoring is limited.

GLEASON SCORING

After the TRUS guided biopsy is done the tissue is stained and subjected to histologic examination. Gleason scoring is done for grading of the two most common patterns of the cells from a score of 1 (lowest) to 5 (highest) and adding them to yield a score with a maximum of 10 and scores above 7 are considered adverse and as high risk towards prostate cancer. Scores of 6 or below is generally considered as low risk for malignancy while a score of 7 is considered as intermediate risk. The higher the Gleason score, the greater is the aggressiveness of the cancer.

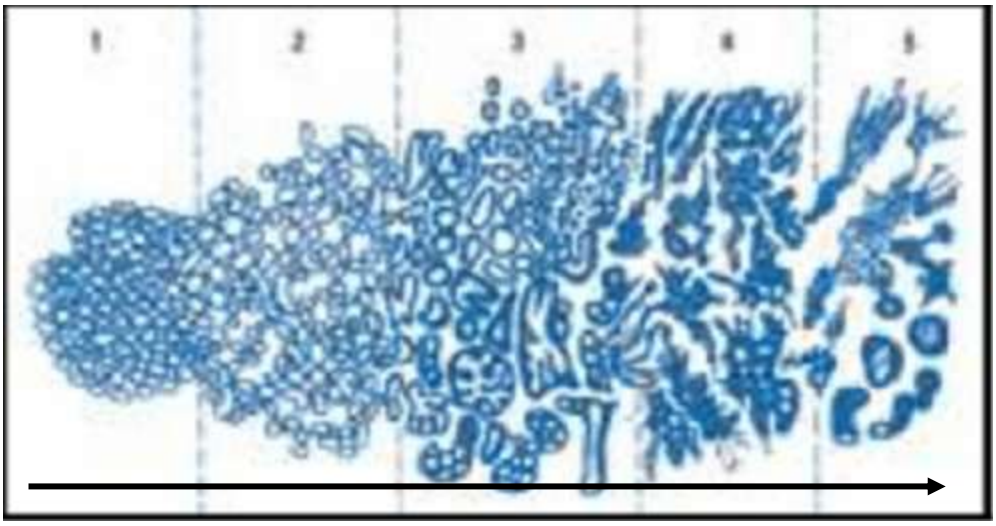

Figure 8.Gleason scoring pattern: Grade 1 to 5

Sometimes, the histologic examination may reveal a total score of 7 which is towards the malignant end of the spectrum. But more important is the separate scores of 2 predominant cell patterns. For example a total a score of 7 may be a 4+3 type or a 3+4 type. In this

case, the 4+3 type cancer pattern is more aggressive than the 3+4 type. Hence, besides the total score the subcomponent score is also important.

RESEARCH STUDIES ON MULTIPARAMETRIC MRI IN PROSTATE CANCER

Prando A et al [97] studied the diagnostic efficacy of tumor apparent diffusion co-efficient (ADC) in correlation with Gleason score and percentage of tumor on core biopsy especially in the peripheral zone prostate cancers using the diffusion-weighted MRI.

The mean ADC for disease with Gleason score 6 was $0.860 \times 10^{(-3)}$ mm^2/s with standard error of 0.036 while with Gleason score 7 it was $0.702 \times 10^{(-3)}$ mm^2/s with standard error of 0.030.

The mean ADC for disease with Gleason score 8 and 9 was $0.672 \times 10^{(-3)}$ mm^2/s and $0.686 \times 10^{(-3)}$ mm^2/s respectively. This differences in the mean ADC values between Gleason score 6 vs 7 and Gleason score 6 vs 8 was statistically significant ($p = 0.0460$).Moreover there was decrease in mean ADC values of 0.006 for every 1% increase in tumor in the core biopsy specimen.

Hence they concluded that DWI can help to differentiate between low-risk Gleason score of 6 and intermediate-risk Gleason score of 7 and low-risk Gleason score of 6 and high-risk Gleason score of 7.

Fehr et al [98] studied the classification of prostate cancers using Gleason scores from Multiparametric MRI images especially the texture

based features of apparent diffusion co-efficient (ADC) and T2 weihted imaging.

They claimed that this texture based classification of the tumours using ADC and T2 weighted images produced 93% accuracy for distinguishing cancers with GS 7 (4 + 3) and those with GS 7 (3 + 4) in the peripheral and the transition zone.

Ouzanne A et al [99] studied the role of combined Multiparametric MRI and targeted biopsies in cases for detection, staging, and grading of anterior prostate cancer (APC). They found that cancer was not detected in 46% of cases by systematic biopsies while only 54% of cases were detected.

The median cancer length of the most involved core in the targeted biopsy was 8mm against 1mm obtained from systematic biopsies ($p < 0.001$). Significant Gleason score upgrading was found in 44% of the cases.

Delongchamps NB et al [100] studied the role of multi-parametric MRI in predicting tumor focality, size and staging in patients with unilateral low-risk prostate cancer. The tumor foci of $>0.2cm^3$ was identified for pathological analysis and these were matched with MRI findings.

They observed that for the tumor detection in the peripheral zone, T2w + DWI + DCE was better significantly than T2w + DWI alone ($p<0.001$) and also in the transition zone, T2w + DWI was better than T2w alone ($p<0.02$). They concluded that with optimum multi-parametric MRI combinations, tumor size was correctly estimated in 77% of cases and about 80% of the bilateral cancers were detected.

They concluded that in the patients with low risk unilateral cancer, Multi-parametric MRI can be used to rule out bilateral involvement an also may be of very good prognostic value.

de Rooij M et al [101] did a meta-analysis of studies for the accuracy of multi-parametric MRI for their use in detection of prostate cancer. About 7 studies which met the inclusion criteria with 526 patients were analysed.

The study showed that multi-parametric MRI had a specificity of 88% with a sensitivity of 74% for prostate cancer detection. Moreover the negative predictive value was in the range of 66% to 81%. Hence the high specificity but variable and high NPV and sensitivity shows the potential role of multiparametric MRI in the detection of prostate cancer.

Citak E et al [102] tried to predict the final Gleason score based on the pre-operative multiparametric MRI (3 Tesla) using the linear discriminant analysis (LDA) and support vector machine (SVM).

Using a standard principal component analysis before Gleason classification, the sensitivity was 51.19% and 64.37% with specificities of 72.7% and 39.9% for LDA and SVM, respectively. They concluded that the SVM classifier resulted in a slightly higher sensitivity but low specificity than LDA for final Gleason score prediction.

Arsov C et al [103] studied the risk of Gleason score upgrading on radical prostatectomy by using the multiparametric MRI targeted and MR-guided biopsy. They observed that in comparison to the TRUS guided biopsy, MR-guided biopsy alone showed low rates of upgrading the conventional Gleason score and the highest Gleason pattern.

The combination of both TRUS-guided and the MR-guided biopsy gave the lowest rate of upgrading. They concluded that multi-parametric MRI is useful tool to characterize and stage the extent of the diasease in the prognostic front.

Siddiqui MM et al [104] also studied the upgrading of prostate cancer using fusion biopsy (MR + Ultrasound) and comparing it with 12 core TRUS biopsy.

The diagnosis of prostate cancer was made in 54% of cases. The addition of targeted biopsy led to upgrading in 32% of cases.

On multivariate analysis, multi-parametric MRI suspicion was associated with Gleason score upgrading in the targeted lesions ($p<0.001$).

Hambrock T et al[105] made an assessment of aggressiveness of carcinoma prostate using MRI guided biopsies versus a systematic 10 core TRUS guided biopsy cohort.

Based on their observations prospectively, they concluded that the diffusion weighted MR- guided biopsies improves the pre-treatment risk stratification by obtaining biopsies which are representative of the actual Gleason score.

Mowatt G et al [106] did a systematic review and an economic evaluation on the diagnostic accuracy and cost-effectiveness of MR spectroscopy (MRSI) and enhanced MRI techniques (DCE and DWI) for localizing the abnormalities of prostate for biopsy.

They concluded that MRSI had high sensitivity and specificity than the T2-MRI. If MRSI and DWI has shown high sensitivity for detection of moderate to high risk patients and also at the same time negates patients with no or low risk of cancer towards undergoing biopsy, then in that case these imaging techniques will be cost-effective.

Schoots IG et al [107] did a systematic review and meta-analysis on the diagnostic accuracy of MR imaging targeted biopsy of prostate versus a standard TRUS guided biopsy and found that there was no significant difference in the overall prostate cancer detection rate between the two techniques although MR-guided biopsy of prostate had a higher rate of detection of significant cancer than the conventional TRUS guided biopsy.

It also had a lower rate of detection of insignificant prostate cancer in comparison to TRUS biopsy and hence recommended the benefits of MR-guided biopsy for detection of prostate cancer at the early stage.

Tonttila P et al [108] did a prospective randomized blinded controlled trial for the use of multi-parametric MRI as a diagnostic tool for detection of prostate cancer in the biopsy-negative men with suspected cancer from the elevated PSA levels.

The trial involved 130 men with elevated levels of PSA randomized to either the MP-MRI group were a pre-biopsy multi-parametric MRI was done followed by a 10 to 12 core TRUS guided biopsy and a targeted fusion biopsy or the control group which underwent only TRUS guided random biopsy.

There was no significant difference in the cancer detection rate between the 2 groups and hence they concluded that diagnostic accuracy of multi-parametric MRI was similar to that of the conventional TRUS biopsy and hence does not provide significant diagnostic advantage over the existing system of TRUS guided biopsy.

Kumar V et al [109]. in 2007 calculated mean ADC value for healthy peripheral zone of the prostate and cancer tissue using pelvic phased array coil on 1.5 Tesla machine. According to this study, mean ADC value (x 10-3 mm2/s) for a healthy peripheral zone of the prostate was found to be 1.80 ± 0.27 and that for cancer tissue was 1.02 ± 0.25.

Later **Nagayama M et al** [110]. in 2011 calculated mean ADC value to differentiate normal and cancerous tissue in peripheral and transitional zones separately. According to this study, the mean ADC values (x 10-3 mm2/s) of cancer lesions and normal tissues were 1.07 ± 0.35 and 1.94 ± 0.31 respectively, in the peripheral zone and 1.00 ± 0.22 and 1.56 ± 0.14 respectively in the transition zone.

There is no single cutoff ADC value to differentiate prostatic cancer from normal tissue, as it depends on many variables, including age [32],MR field strength, b value[111]. coil employed, overlap of ADC values between healthy and cancerous tissues[112]. and location of cancer within the gland[113]. There are only few studies that have compared the

relationship between ADC values with Gleason‘s score which predicts tumor aggressiveness.

Yoshimitsu K et al [114] in 2008 and Verma S et al [115]. in 2011compared ADC values with Gleason‘s score derived from radical prostatectomy specimens and found that there was significant decrease in ADC values with increasing Gleason‘s score.

Another study by **Woodfield CA et al**[116]. in 2010 and Yagci AB et al[117]. in 2011 compared ADC values with Gleason score derived from core biopsy specimens and also described a decrease in ADC values with increasing Gleason‘s score.

In addition, **Woodfield CA et al** [116]. also established an inverse relationship between ADC values and the percentage of tumor involvement on prostate core biopsies.

A similar studies by Luczynska E et al [118] and Anwar SS et al [119] in 2014 also reported DWI can differentiate patients with prostate cancer into low, intermediate and high risk groups but used pelvic phased array coil for imaging.

DeCobelli F et al [120] in 2015 prospectively analyzed 72 patients who underwent ultrasound guided sextant biopsy and magnetic resonance imaging of the pelvis using endorectal coil on 1.5 Tesla machine. DWI was done using b values 0, 800 and 1600 s/mm2.

The paper reported mean tumor ADC values may help to differentiate between low-risk (Gleason‘s score <6), intermediate-risk (Gleason‘s score =7), and high-risk (Gleason‘s score >7) prostate cancers, and thereby indirectly can determine the aggressiveness of the disease.

Mean ADC value was 0.96 x 10-3 mm2/s for tumors with Gleason‘s score 6, 0.80 x 10-3 mm2/s for tumors with Gleason‘s score 7 and 0.78 x 10-3 mm2/s for tumors with Gleason‘s score 8-10.

Hoeks et al [121] reviewed the multi-parametric MR imaging techniques for its use in the localization, detection and staging of prostate cancer and concluded that although the reported accuracies of separate and combined multi-parametric MR imaging are variable from study to study and also based on the technical specifications and clinical indications, multi-parametric MR imaging has shown great promise both in the diagnostic as well as in the prognostic front.

The major limiting factor towards the use of multi-parametric MR imaging above and beyond the cost factor is the absence of consensus over technical approaches like field strengths, sequences, use of endorectal coils and also absence of guidelines for indications of use of multi-parametric MRI precludes its use in place of the much used TRUS imaging. Also computer programs which allow for evaluation of the individual components of the multi-parametric MRI should be developed.

Moreover, educating the radiologists and ensuring wide availability of multi-parametric MRI techniques poses challenge in the practical aspect. Computer-aided diagnosis out of more complex multi-parametric MR imaging can be fast, reliable, easy and at the same time cost-effective.

Improvisation of the currently existing components of multi-parametric MRI is not very far and probably in the near future other techniques like DTI, MR Elastography, multi-component diffusion analysis and newer spectroscopic methods **Hegde et al** [122] will be added to the existing spectrum.

Table 2. Comparison of mean tumor ADC values (x 10-3 mm2/s) with Gleason's score in prior studies.

	Low risk adenocarcinoma (Gleason's score ≤ 6)	Intermediate risk adenocarcinoma (Gleason's score = 7)	High risk adenocarcinoma (Gleason's score >7)
Yoshimitsu K et al[52] (2008)	1.19	1.10	0.93
Woodfield CA et al[54] (2010)	0.86	0.70	0.68
Yagci AB et al[55] (2011)	1.18	1.05	0.84
Verma S et al[53] (2011)	1.08	1.02	0.90
Luczynska E et al[56] (2014)	0.85	0.72	0.61
Anwar SS et al[57] (2014)	0.93	0.83	0.57
De Cobelli F et al[58] (2015)	0.96	0.80	0.78

MATERIALS AND METHODS

STUDY DESIGN

Prospective observational study. The study was approved by institutional scientific and ethical committee review board.

STUDY PERIOD

November 2016 - June 2017.

SOURCE OF PATIENTS AND RECRUITMENT

Patients reporting with obstructive lower urinary tract symptoms to the Department of Urology in Madras Medical College, Rajiv Gandhi Government General Hospital, Chennai.

PATIENT SELECTION

Inclusion Criteria

- 25 males with age between 50 and 78 years
- Raised Prostate-specific antigen (PSA) levels
- Subjects willing to participate and give informed written consent
- No other comorbidities

Exclusion Criteria

Patients with Urinary tract infections, bleeding disorders, claustrophobia, patients with AUR, & implants were excluded from the study.

PATIENT PREPARATION

Pre-procedural antibiotic in the form of Tab.Ciprofloxacin 500mg 30 minutes prior to procedure and rectal enema was given.

Viral serological tests were done and all the patients were explained about the indications, risks of the procedure and an informed consent was obtained from all the participants.

PATIENT POSITION

Supine position for the MRI sequences and left lateral position for TRUS imaging and biopsy.

IMAGING EXAMINATION

All the 25 patients were subjected for the multi-parametric MRI sequences including T1 and T2 weighted anatomical imaging, functional imaging using diffusion weighted MRI and DCE along with MR spectroscopy.

The machine used in this study is SIEMENS 3.0 Tesla MRI (Skyra, Erlangen Germany) with phased array body coil.

Multi-parametric MR imaging protocol included 2D T2w-MRI, DW-MRI, DCE-MRI and MRSI. High resolution Axial, Sagittal and coronal T2WI using T2w turbo spin echo sequence was taken in three orthogonal planes.

The signal intensities of prostate gland involving lateral lobes, median lobe and peri-urethral glandular region were analyzed.

TABLE 3.PARAMETERS:

MP-MRI	Routine	Resolution
T2 W	TR : 4000 ms TE : 101 ms Slice thickness: 3.0 mm Flip angle : 150º	Fov read: 220mm Fov phase: 100% Base resolution: 320 Phase resolution: 90%
DWI b values : 50,400,800	TR : 3700 ms TE : 68.0 ms Slice thickness: 3.5 mm	Fov read: 200mm Fov phase: 100% Base resolution: 140 Phase resolution: 100%
MR Spectroscopy	TR : 940 ms TE : 145 ms Flip angle : 90º	Fov A > > P : 84mm Fov R > > L : 84mm Fov F > > H : 70mm

MP-MRI	Geometry	Sequence
T2 W	Slices : 20 Matrix : 256 × 256	Band width: 200Hz/Px Echo spacing: 11.2 ms Turbo factor : 25 Echo trains/slice :9
DWI b values : 50,400,800	Slices : 20	Band width: 1190Hz/Px Echo spacing: 0.94 ms EPI factor : 140
MR Spectroscopy	Thickness : 20mm	Band width: 1300Hz/Px Aquisition duration: 393ms Delta frequency: -1.80ppm

PI-RADS SCORING SYSTEM

The prostate imaging- reporting and data system (PI-RADS) was followed in the study. The PI-RADS scoring is based on the European Society for Urogenital Radiology (ESUR) guidelines for uniform structured scoring system for components of multi-parametric MRI.

The PI-RADS scoring system is basically a 5 point Likert scale system of scoring each individual lesion in each component of multi-parametric MRI and the total composite score out of 20 involving all 4 components like T2w-MRI, DWI-MRI, DCE-MRI and MR spectroscopy was calculated to classify the risk of malignancy for the lesion.

TABLE 4.The PI-RADS scoring is as follows:

Score	Criteria
A1	**T2WI for peripheral Zone**
1	Uniform high intensity signal (SI)
2	Linear, wedge shaped or geographic areas of lower signal intensity but not well demarcated
3	Intermediate but not in categories 1 or 2 and 4 or 5
4	Discrete and homogenous low intensity signal focus or mass confined to prostate
5	Discrete and homogenous low intensity signal focus or mass not confined to prostate with extra-capsular extension or broad (1.5cm) contact with surface
A2	**T2WI for Transition Zone**
1	Heterogeneous adenoma with well-defined margins: organized chaos
2	More homogenous areas of low signal but well-marginated

Score	Criteria	
3	Intermediate but not in categories 1 or 2 and 4 or 5	
4	Areas of more homogenous low signal intensity but ill-defined: erased charcoal sign	
5	Same as 4 + involvement of anterior fibromuscular stroma or anterior horn of PZ	
B	Diffusion Weighted imaging (DWI)	
1	No reduction in ADC and no increase in signal intensity in any high value b image (>b800)	
2	Diffuse, hyper-SI on >b800 image with low ADC but no focal features but linear, triangular or geographical features are allowed	
3	Intermediate but not in categories 1 or 2 and 4 or 5	
4	Focal areas of reduced ADC but iso-intense signal on high value b image (>b800)	
5	Focal areas/mass of reduced ADC but hyper-intense signal on high value b image (>b800)	
C	**Dynamic contrast enhanced MRI (DCE)**	
1	Type 1 enhancement curve	
2	Type 2 enhancement curve	
3	Type 3 enhancement curve	
+1	Focal enhancing lesion with curve type 2 or 3	
+1	Asymmetric lesion or lesion at unusual location with curve type 2 or 3	
D1	**Quantitative MRS Choline+ Creatine/citrate ratios**	
Rating	Peripheral zone	Transition zone
1	<0.44	<0.52
2	0.44 – 0.58	0.52 – 0.66
3	0.58 – 0.72	0.66 – 0.80

Score	Criteria	
4	0.72 - 0.86	0.80 – 0.94
5	>0.86	>0.94
D2	**Qualitative MRSI : For adjacent 3 voxels: Pattern analysis**	
1	Citrate peak height exceeds choline peak height >2 times	
2	Citrate peak height exceeds choline peak height >1 but <2 times	
3	Citrate peak height equals choline peak height	
4	Choline peak height exceeds Citrate peak height >1 but <2 times	
5	Choline peak height exceeds Citrate peak height >2 times	

This Total aggregate score of PI-RADS in the study was calculated and was correlated with Gleason score after the tissue biopsy.

TRUS SCAN AND TRUS GUIDED BIOPSY

All the twenty five patients were subjected for TRUS scan with 7 Mhz Aloka machine with rectal probe in left lateral position.

Complete zonal anatomy of prostate was studied and systematic sextant biopsies of 8 core were taken. Each biopsy specimen was specifically labeled according to the orientation of biopsy site and sent for histopathological examination.

All the patients were given one dose of ciprofloxacin 500 mg half an hour prior to TRUS biopsy. All the patients were given low rectal enema prior to biopsy.No patient developed any untoward complication following the procedure.

HISTOPATHOLOGICAL ANALYSIS

Gleason‘s score was obtained by histopathologic analysis of the TRUS guided biopsy specimens. The tumors were then divided into three groups based on Gleason‘s score.

Tumors with Gleason‘s score <6 were categorized as low grade tumors, score equal to 7 as intermediate grade tumors and those with score >7 as high grade tumors.

STATISTICAL ANALYSIS

The collected data were analysed with IBM.SPSS statistics software 23.0 Version. To describe about the data descriptive statistics frequency analysis, percentage analysis were used for categorical variables and the mean & S.D were used for continuous variables.

To find the agreement between PI-RADS & Gleason's score the Inter rater reliability Cohen's Kappa was used.

For the multivariate analysis the Kruskal Walli's test followed by the Mann-Whitney U test was used. To assess the relationship between the variables Spearman's rank Correlation was used.

The sensitivity, specificity, positive predictive value (PPV) and negative predictive value (NPV) of DWI were computed for low grade (GS <6), intermediate grade (GS =7) and high grade (GS >7) tumors.

Kappa value was also calculated for individual tumor grades which measures inter-rater agreement for categorical variable.

Kappa value of <0 falls under less than chance agreement, 0.01 – 0.20 – slight agreement, 0.21 – 0.40 – fair agreement, 0.41 – 0.60 – moderate agreement, 0.61 – 0.80 – substantial agreement and 0.81 – 0.99 – almost perfect agreement.

Spearman‘s correlation was used to assess the relationship between two variables. In all the above statistical tools the probability value 0.05 is considered as significant level.

TABLE 5.

Kappa value	Interpretation
< 0	Poor agreement
0.0 – 0.20	Slight agreement
0.21 – 0.40	Fair agreement
0.41 – 0.60	Moderate agreement
0.61 – 0.80	Substantial agreement
0.81 – 1.00	Almost perfect agreement

OBSERVATION AND RESULTS

A total of 25 participants were included in the study.Mean age group and standard deviation were found to be 68.96 ± 8.682 with a range of 50–83 years. The majority of the participants were in the sixth and seventh decade of life as shown in the Table 6.

The mean ± SD serum PSA level was 53.06 ± 40.32, range 5.5-110 ng/ml. Participant‘s demographic and clinical data were summarized in Table 6.

The Gleason sum score ranged from 6 to 9 for malignant tissues reported by TRUS biopsy.

Table 6: Descriptive statistics of various parameters

Parameters	Mean	Median ± SD	Minimum	Maximum
Age	68.96	69.00 ± 8.68	50	83
Prostate volume (cc)	50.4	45.00 ± 19.0	30	100
PSA(ng/ml)	53.06	38.00 ± 40.32	5.5	110
ADC	0.71	0.72 ± 0.10	0.46	0.87

Table 7: Classification of multiparametric-MRI PIRADS score

PIRADS score	Frequency	Percent
Highly Suspicious malignancy	11	44.0
Probably Malignant	11	44.0
Indeterminate	3	12.0
Total	**25**	**100**

Fig 9: Pie chart showing distribution of PI-RADS score of malignant lesions in TRUS biopsy

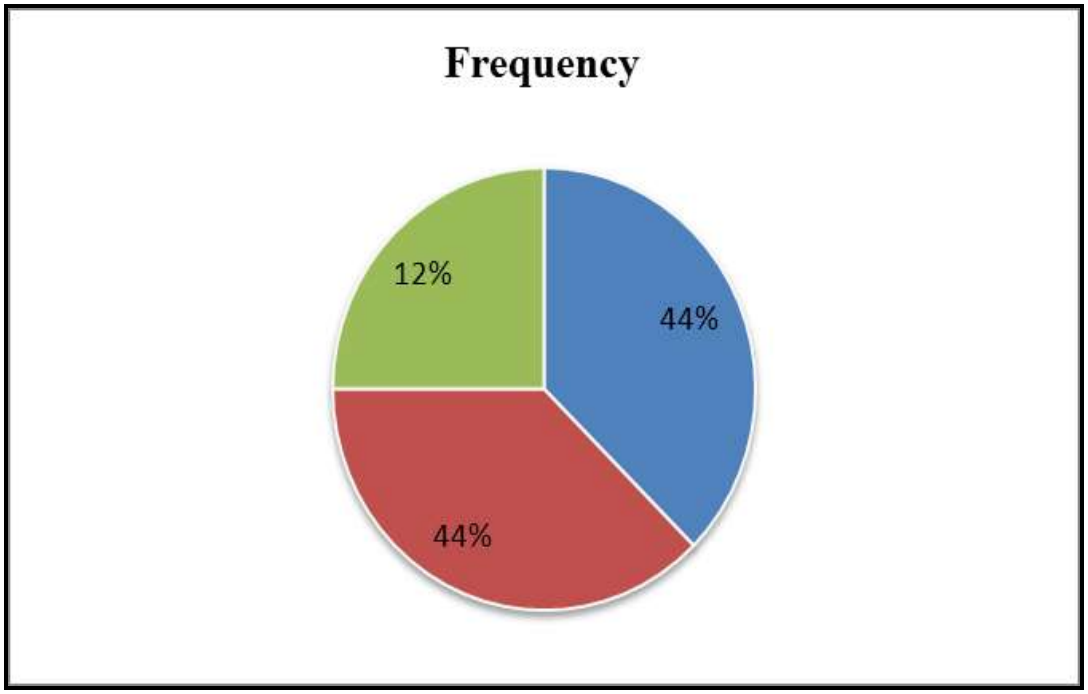

Table 8: Distribution of Gleason Score of the malignancies in TRUS biopsy

Gleason sum Score	Frequency	Percentage
9	6	24%
8	5	20%
7	8	32%
6	6	24%
Total	**25**	**100%**

Fig 10: Pie chart showing distribution of Gleason's score of malignant lesions in TRUS biopsy

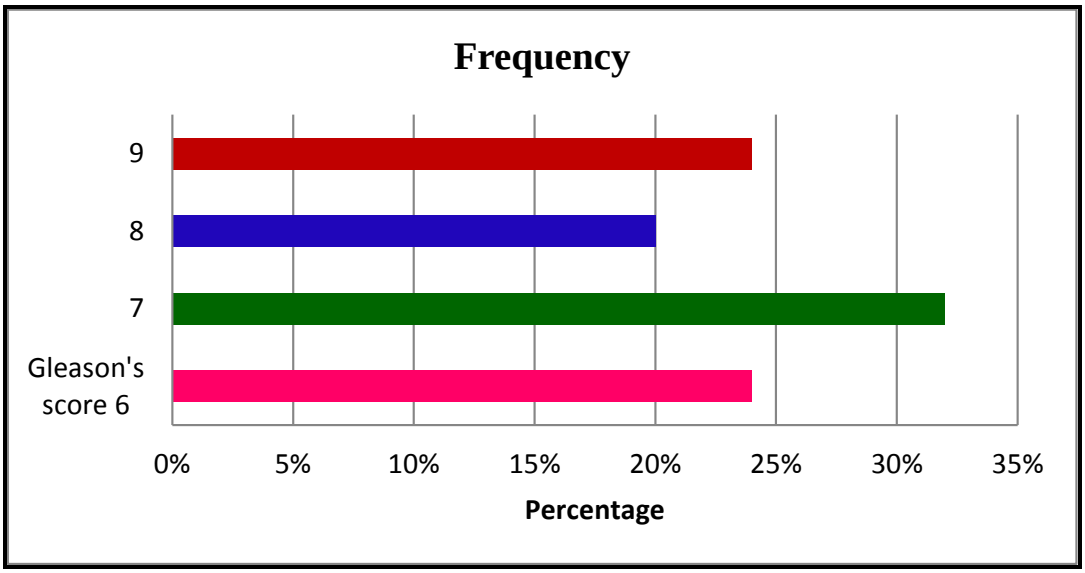

Table 9. Participant's histopathological data considered in the study population (n = 25).

Grade	Gleason's score	Frequency	Percentage
Low	≤ 6 (3+3)	6	24%
Intermediate	= 7		
	(3+4)	5	20%
	(4+3)	3	12%
High	> 7		
	8 (4+4)	3	12%
	(5+3)	2	8%
	9 (5+4)	6	24%
Total		**25**	**100**

Table 10. Comparison of mean,minimum and maximum tumor ADC values (x $10^{-3}mm^2/s$) between three Gleason groups.

	No. of participants	**Mean ADC ± SD**	**Minimum ADC**	**Maximum ADC**	**P value**
Gleason's score ≤ 6	6	0.85 ± 0.02	0.81	0.87	<0.001
Gleason's score = 7	8	0.74 ± 0.02	0.71	0.77	
Gleason's score > 7	11	0.63 ± 0.08	0.46	0.74	

Table 11. Summary of the relationship between mean tumor ADC values with Gleason's score.

Spearman's correlation		Gleason's score
Mean tumor ADC	Correlation coefficient	- 0.912
	p value	<0.001
	No. of participants	25

Fig.11. Summary of the relationship between mean tumor ADC values with Gleason's score.

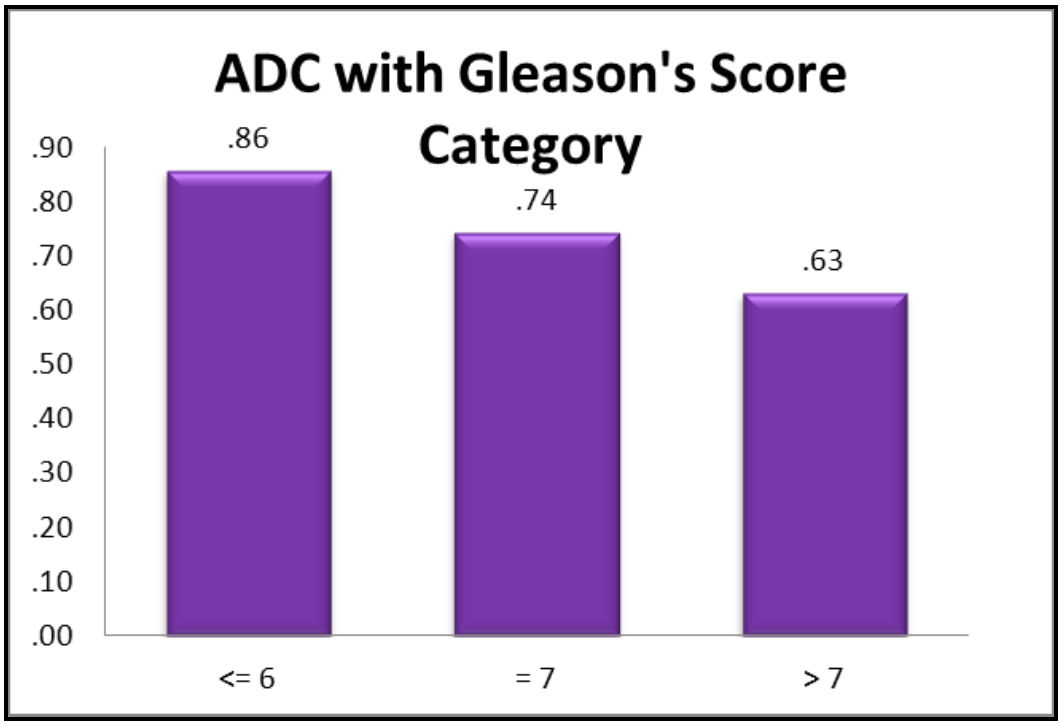

Fig.12 Summary of the relationship between mean tumor ADC values with Gleason's score.

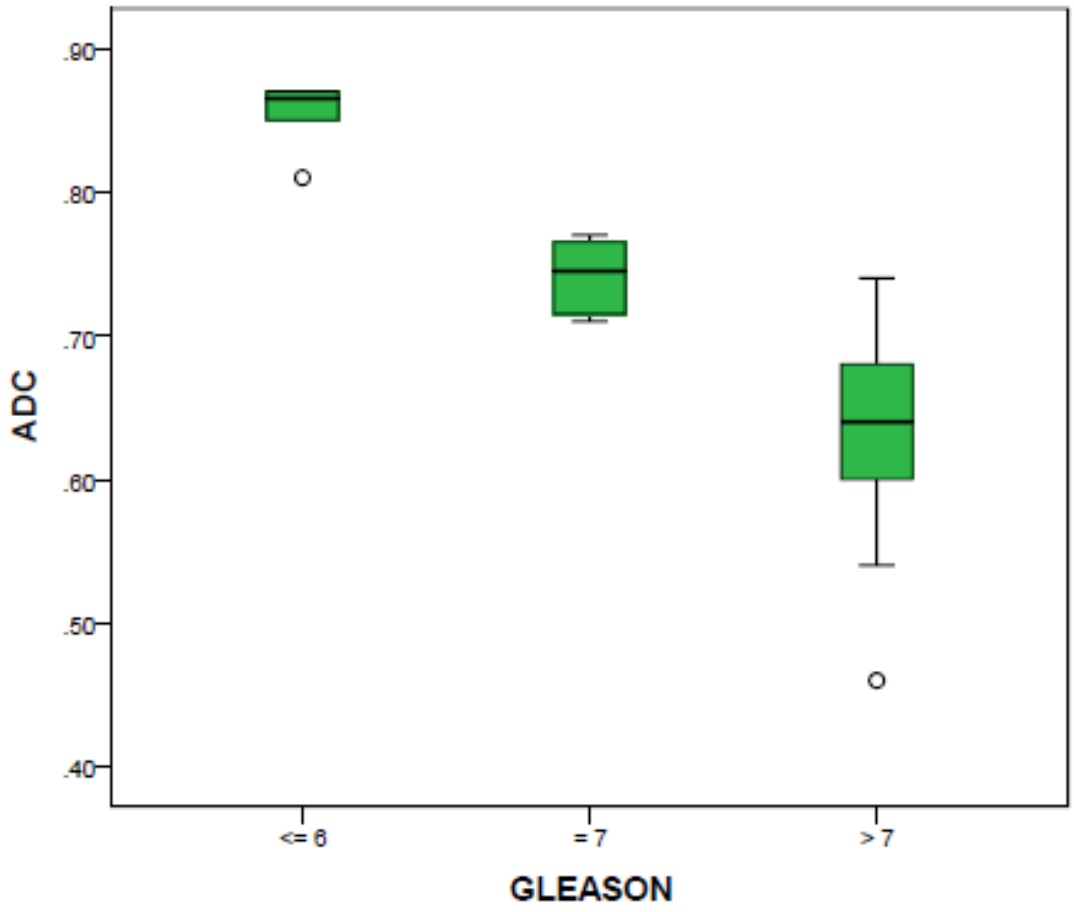

Table 12. Summary of the relationship between PI-RADS score with Gleason's score.

Spearman's correlation		**Gleason's score**
PI-RADS	Correlation coefficient	+ 0.790
	p value	<0.001
	No. of participants	25

Fig.13 Summary of the relationship between PI-RADS score with Gleason's score.

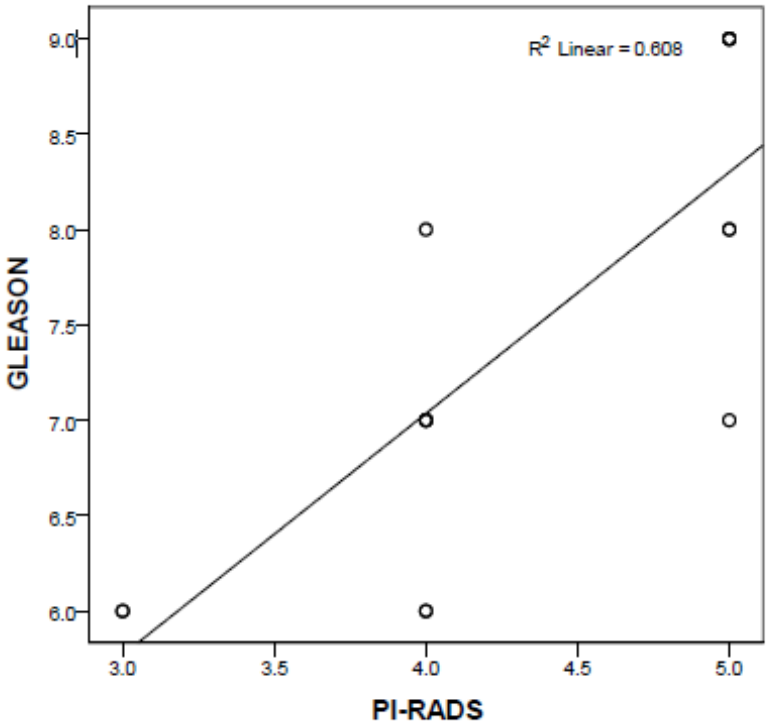

Table 13. Summary of sensitivity, specificity, positive predictive value, negative predictive value and kappa value for PI-RADS Vs Gleason's sum score.

PI-RADS Score	Gleason's score	Sensitivity %	Specificity %	PPV %	NPV %	Kappa value	P-value
3	< = 6	50	100	100	86.4	0.60	0.001 **
4	7	75	70.6	54.5	85.7	0.42	0.032 *
5	> 7	81.8	85.7	81.8	85.7	0.68	0.001 **
Overall accuracy		68.9	85.4	78.8	85.9	0.56	
** Highly Sig. at P < 0.01 level & * Sig. at P < 0.05 level							

DISCUSSION

The age of the patients in the current study ranged from 50 to 83 years, with a mean age of 68.96 ± 8.6 years. The majority of the participants were in the sixth and seventh decade of life as shown in the Table 6.

The mean ± SD serum PSA level was 53.06 ± 40.32, range 5.5-110 ng/ml. Participant‘s demographic and clinical data were summarized in Table 6.

Out of the 25 patients subjected for TRUS biopsy about 6 patients reported a Gleason score of 6 , 8 patients reported a Gleason score of 7 and 11 patients reported a Gleason score of 8 & above indicating in favor of Malignancy as shown in the Table 8.

In our study, out of 25 patients subjected for TRUS biopsy about 3 patients reported a PIRADS score of 3, 11 patients reported a PIRADS score of 4 & 11 patients reported a PIRADS score of 5 indicating malignancy as shown in the Table 9.

Magnetic resonance imaging (MRI) is a commonly used imaging technique to diagnose and stage the prostate cancer. The introduction of more conservative treatment options and increasing number of indolent

tumors has increased the need for better characterization of tumor aggressiveness to choose the appropriate treatment.

Since trans-rectal guided tumor biopsies are invasive and do not accurately classify Gleason‘s score in approximately 38% of all tumors [(123)] due to sampling errors, the value of multi-parametric MRI as a non-invasive tool to predict tumor aggressiveness has been under investigation.

In multi-parametric prostate study, functional imaging techniques such as diffusion weighted imaging, dynamic contrast enhanced imaging and MR spectroscopy are used to detect prostate cancer. Diffusion weighted imaging is the only functional imaging technique that can assess the diffusion of proton molecules in vivo and provides information about the biological properties of tissue.

Diffusion weighted imaging has numerous advantages over other MR techniques such as short acquisition time, less subjective signal interpretation as compared to T2 weighted and dynamic contrast enhanced imaging[(124)] and less partial volume effects than MR spectroscopy.

Parallel imaging technique further improves the quality of DWI by reducing the sampling time, reducing motion artifacts, decreasing the

number of gradient echoes and reducing magnetic susceptibility artifacts.

Neoplastic tissues are characterized by increased cell density with decreased extracellular space, thereby reducing the diffusion of free water molecules resulting in restricted diffusion.

In evaluating the relationship between ADC value and tumor aggressiveness, we found that there is a significant decrease in ADC value with increasing Gleason‘s score as reported by previous studies [114-120].

This finding suggests an inverse relationship between ADC value and tumor aggressiveness with reference to biopsy Gleason‘s score. This can be explained by an increase in cellular density in high grade tumors resulting in more restricted diffusion of water molecules as established by Zelhof B et al [125].

Our study also showed that mean ADC value of tumors with Gleason‘s score <6 was significantly different from the tumors with Gleason‘s score =7 and Gleason‘s score >7. The difference in mean ADC value of tumors with Gleason‘s score =7 and Gleason‘s score >7 were also found to be statistically significant.

This suggests that mean ADC value could differentiate between low risk (GS <6), intermediate risk (GS =7) and high risk tumors (GS >7), provided the tumor is visible on DWI.

In our study, mean ADC for tumors with Gleason's score of <6 was 0.85 ± 0.02 x 10^{-3} mm^2/s , Gleason's score of 7 was 0.74 ± 0.02 x 10^{-3} mm^2/s and Gleason's score >7 was 0.63 ± 0.08 x 10^{-3} mm^2/s.

In contrast, previous studies estimating the significance of differences in mean ADC values between the three groups had shown variable results.

Earlier studies by Yoshimitsu K et al[114] and Woodfield CA et al[116]on peripheral zone prostatic cancers showed that mean ADC values could differentiate only the low risk tumors from high risk tumors, but there was no statistically significant difference in mean ADC value between low risk and intermediate risk tumors and between intermediate risk and high risk tumors.

Yoshimitsu K et al[114] used pelvic phased array coil for DWI with b values of 0, 800 and 1000 and mean ADC for tumors with Gleason's score of <6 was 1.19 ± 0.15 x 10^{-3} mm^2/s, Gleason's score of 7 was 1.10 ± 0.24 x 10^{-3} mm^2/s and Gleason's score >7 was 0.93 ± 0.20 x 10^{-3} mm^2/s.

Woodfield CA et al[116] used endo-rectal coil for imaging with b values of 0 and 1000 and mean ADC for tumors with Gleason's score of <6 was 0.86 ± 0.04 x 10^{-3} mm^2/s Gleason's score of 7 was 0.70 ± 0.02 x 10^{-3} mm^2/s and Gleason's score >7 was 0.68 ± 0.02 x 10^{-3} mm^2/s.

Yagci AB et al [117] studied peripheral zone prostatic cancer using endo-rectal coil and b values of 0 and 800. The study showed that there was significant decrease in ADC value with increase in tumor grade and mean ADC for tumors with Gleason's score of <6 was 1.18 ± 0.44 x 10^{-3} mm^2/s Gleason's score of 7 was 1.05 ± 0.15 x 10^{-3} mm^2/s and Gleason's score >7 was 0.84 ± 0.16 x 10^{-3} mm^2/s.

Luczynska E et al [118] used pelvic phased array coil for imaging with b values of 0, 100, 300, 800 and 1000. The study showed that DWI may be helpful in differentiating high grade tumors from intermediate and low grade tumors and mean ADC for tumors with Gleason's score of <6 was 0.85 ± 0.03 x 10^{-3} mm^2/s Gleason's score of 7 was 0.72 ± 0.03 x 10^{-3} mm^2/s and Gleason's score >7 was 0.61 ± 0.04 x 10^{-3} mm^2/s.

Anwar SS et al [119] also studied peripheral zone prostatic cancer using pelvic phased array coil with b values of 0, 400 and 800 and showed that mean ADC values could differentiate between low risk (GS <6) and high risk (GS >7) tumors and between intermediate risk (GS =7) and high risk (GS >7) tumors.

But the differentiation between low risk and intermediate risk tumors was found to be statistically insignificant. According to this study, mean ADC for tumors with Gleason‘s score of <6 was 0.93 ± 0.20 x 10^{-3} mm^2/s.Gleason‘s score of 7 was 0.83 ± 0.12 x 10^{-3} mm^2/s.and Gleason‘s score >7 was 0.57 ± 0.15 x 10^{-3} mm^2/s.

All these studies were conducted on a 1.5 Tesla magnet, but used different b values and imaging parameters for DWI with or without endorectal coil, which might be the reason for discrepant results between the individual studies.

Woodfield CA et al[(116)]. studied the relationship between mean tumor ADC values and the percentage of tumor involvement on prostate core biopsy specimens and found that there was a decrease in mean tumor ADC values with increasing percentage of tumor involvement, which is similar to the results of our study. The decrease in ADC values is partly due to better visibility of lesions on DWI and ADC maps with increasing tumor volume when compared to the less dense tumor, thereby facilitating larger and more accurate placement of ROI on ADC maps.

GLEASON’S SCORE

6 (24.0%) out of 25 participants had a Gleason‘s score of 6 (GS 3+3), 8 (32.0 %) participants had a Gleason‘s score of 7 (5 participants had GS 3+4 and 3 had GS 4+3) and 11 (44.0 %) participants had a

Gleason‘s score >7 (3 participants had GS 4+4, 6 had GS 5+4 and 2 had GS 5+3) as shown in Table 9.

There was a positive linear correlation between PIRADS score and Gleason score (+0.790) with p value <0.001 i.e. increase in levels of PIRADS score is associated with a corresponding increase in levels of Gleason score in raised PSA levels. The positive linear correlation between PIRADS score and Gleason score was statistically significant, it indicates that among the patients who tested positive for malignancy in TRUS biopsy, the higher the Gleason sum score the higher the PIRADS score and hence role of MP-MRI in characterizing the extent and aggressiveness of the malignancy is revealed. This is an added advantage especially in cases of pre-biopsy MRI as it may help in targeted biopsy and also targeted therapy which limits the recurrence and also provides better guidance for complete surgical clearance.

On the other hand, Mean ADC value of tumors decreased progressively with increasing Gleason‘s score as shown in Table 5 and Figure 10 & 11.

The correlation coefficient between mean tumor ADC values and Gleason‘s score was – 0.912 with p value <0.001 as shown in Table 11.

The correlation between multi-parametric MRI based PIRADS and Gleason score had a sensitivity of around 68.9% and a specificity of

85.4%. The specificity of multi-parametric MRI is also on the higher side indicating its potential in eliminating the patients who would otherwise undergo TRUS biopsy for a negative result. Therefore, unwanted and unnecessary biopsies can be avoided using multi-parametric MRI and hence reducing the patient discomfort and unnecessary burden on the health system.

Moreover the positive predictive value was 78.8%, while the negative predictive value was 85.9%. The high negative predictive value indicates the post-test probability of a patient with negative results in multi-parametric MRI to have a malignant lesion is literally zero.

The accuracy of a diagnostic test, in this case multi-parametric MRI is the ability of the test to correctly diagnose those with disease and exclude those without the disease. Hence the role of multi-parametric MRI in patients especially with raised PSA levels in deciding whether to go for TRUS biopsy is significant.

According to the classification of multi-parametric-MRI based PIRADS score, about 44% of the patients had highly suspicious malignancy and about 44% had a probably malignant lesion while 12% of the patients had indeterminate lesions.

Studies have shown that because of the low predictive value of TRUS it is not recommended as a first-line screening test for early prostate cancer[126-128].

The effectiveness of PSA as a screening method for early diagnosis of prostate cancer is debated in the last decade. However, it has been proved that use of PSA increases detection rates of prostate cancer and leads to the detection of prostate cancers that are more likely to be confined when compared with detection without the use of PSA. This has been documented in population-based data, observational studies, and randomized screening trials.

The choice of a PSA threshold or cut point above which one would recommend further evaluation to rule out prostate cancer in the form of prostate biopsy using TRUS is controversial[129-131]. The controversy is that the use of higher PSA thresholds risks missing an important cancer until it is too late for a cure, whereas the use of lower PSA thresholds increases not only unnecessary biopsies but also the proportion of biopsies that identify clinically insignificant disease like disease that would not have been detected in the absence of screening.

A number of studies have confirmed the inability of TRUS to localize early prostate cancer[132,133] So to avoid unnecessary TRUS biopsies and at the same time detecting carcinoma in patients with grey zone PSA is a challenging task.

Many studies have shown that the TRUS biopsies are limited by a low sensitivity of 60%, a PPV of only 25% and false-negative rate estimated to be as high as 15–34% [134,135]. Combining MRI with TRUS-guided biopsy could help in (i) directing biopsy to the suspicious area and therefore improve its detection rate, and (ii) avoiding the biopsy in those who have no suspicious lesions and therefore avoiding all risks associated with an invasive biopsy.

The research studies prospectively evaluating the role of MRI in men with a PSA level of < 10 ng/mL, who have poorest cancer detection rate and the highest false-negative rate on TRUS biopsy found a cancer detection rate about three times better, and a NPV approaching 100%[136,137]. Similar negative predictive value was obtained in this study also.

This study findings are similar to Delongchamps NB et al [100] were the tumor size was correctly estimated in 77% of cases and about 80% of the bilateral cancers were detected and also multiparametric MRI can be used to rule out bilateral involvement and also of very good prognostic value.

Similar findings were observed by de Rooij M et al [101] in a meta-analysis of studies for the accuracy of multiparametric MRI which showed a specificity of 88% and a sensitivity of 74% for multi-parametric MRI in prostate cancer detection. Moreover the negative

predictive value was in the ranged from 66% to 81% in the above stated study.

The sensitivity and specificity of multi-parametric MRI observed in this study was higher than that of one observed by Citak E et al [102] as they tried to predict the final Gleason score based on the pre-operative multi-parametric MRI (3 Tesla) using the linear discriminant analysis (LDA) and support vector machine (SVM). Using a standard principal component analysis before Gleason classification, the sensitivity was 51.19% and 64.37% with specificities of 72.7% and 39.9% for LDA and SVM, respectively. They concluded that the SVM classifier resulted in a slightly higher sensitivity but low specificity than LDA.

Mowatt G et al [106] did a systematic review and an economic evaluation on the diagnostic accuracy and cost-effectiveness of MR spectroscopy (MRSI) and enhanced MRI techniques (DCE and DWI) for localizing the prostate abnormalities for biopsy. They observed that sensitivity was highest for MRSI at 92% while TRUS imaging had a high specificity of 81%. They concluded that MRSI had high sensitivity and specificity than the T2-MRI. If MRSI and DWI has shown high sensitivity for detection of moderate to high risk patients and also at the same time negates patients with no or low risk of cancer towards undergoing biopsy, then in that case these imaging techniques will be cost-effective.

Based on these study findings, it can be safely said that multiparametric MRI PIRADS has positive correlation with Gleason and ADC has negative correlation with Gleason with high sensitivity and specificity with better predictive values and hence pre-biopsy multi-parametric MRI can serve as not only as a screening tool but also a valuable diagnostic investigation providing assistance for guided and targeted biopsy besides having the ability to characterize the extent and aggressiveness of the prostate cancer at the earliest that too non-invasively.

Moreover, application of multi-parametric MRI PIRADS scoring in individuals with elevated PSA levels can lead to reduction in number of negative biopsies and thereby reducing patient discomfort and unwanted expenditure. It can be concluded that multi-parametric MRI PIRADS scoring can play a significant role not only in screening for prostate cancer but also in the diagnosis, treatment and in the prognostic front.

LIMITATIONS

There are few limitations in this study. First, sextant based TRUS biopsy was used as the reference standard for comparing ADC values with Gleason‘s score rather than step section histopathology of radical prostatectomy specimens. Gleason‘s score derived from histopathological analysis of radical prostatectomy specimens may differ from TRUS guided biopsy derived Gleason‘s score and there may be 20-30% upstaging of Gleason‘s score from core biopsy to radical prostatectomy specimens[85] .

TRUS guided biopsies could miss small tumor focus visible on MR imaging, making it less accurate for diagnosis. The false negative rate of standard sextant biopsy is around 39%[86] . Absolute sextantmatching of the prostate on TRUS guided biopsy and MRI is subjective and is prone to errors. Second, the ADC values are influenced by the degree of diffusion sensitization (b-value) used in the study.

In our study, we used b values of 50, 400 and 800 s/mm^2 and the mean ADC values for tumors with GS <6, GS =7 and GS >7 obtained in our study may not be the same as that obtained in other studies with different b values.

CASE 1

Case of prostatic adenocarcinoma with Gleason score 6 (3+3) vs PI-RADS 3.

T2 weighted

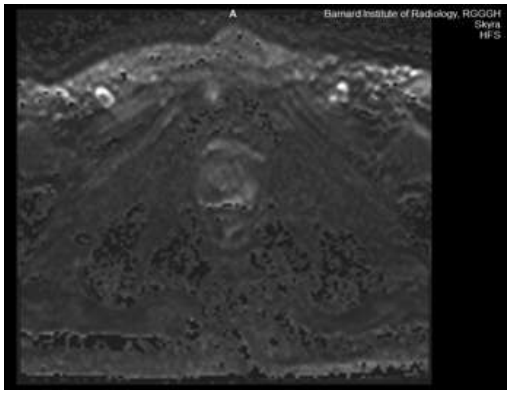

Diffusion Weighted

ADC

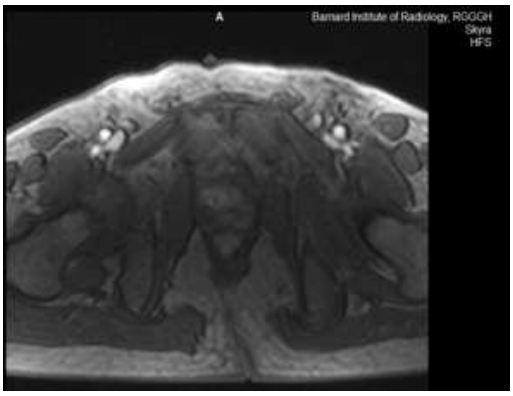

Post Contrast

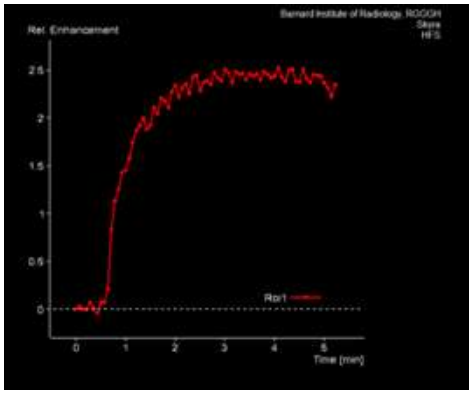

Time Intensity Curve

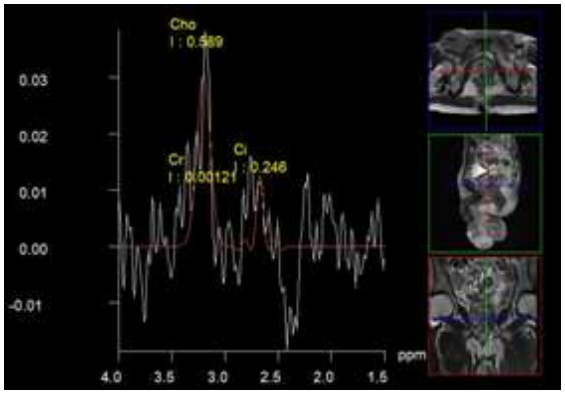

MR Spectroscopy

MRI Axial T2W, Diffusion, ADC images shows an ill-defined, non- circumscribed moderate hypointense nodule in the peripheral zone of left apex of prostate.

On DWI, the nodule shows restricted diffusion with low ADC value on ADC map. ADC value: 0.851 x 10^{-3} mm^2/s. Dynamic contrast image shows minimal focal enhancement and Type II plateau pattern curve. MRS shows increased choline integral values.

CASE 2

Case of prostatic adenocarcinoma with Gleason score 7 (4+3) vs PI-RADS 4.

T2 Weighted

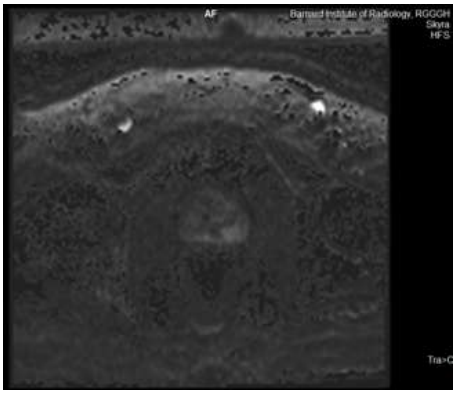

Diffusion Weighted

ADC

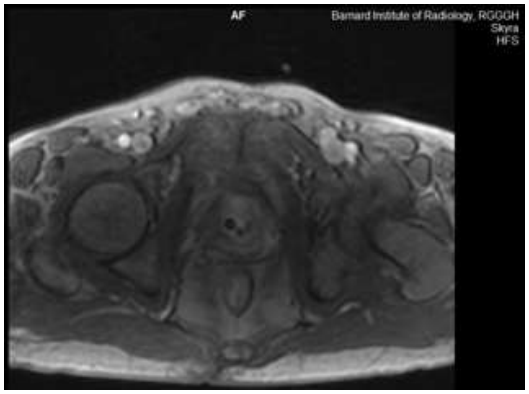

Post Contrast

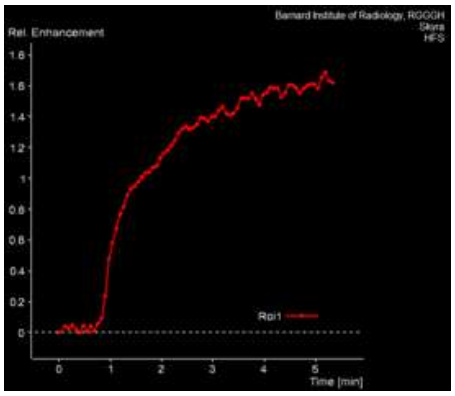

Time Intensity Curve

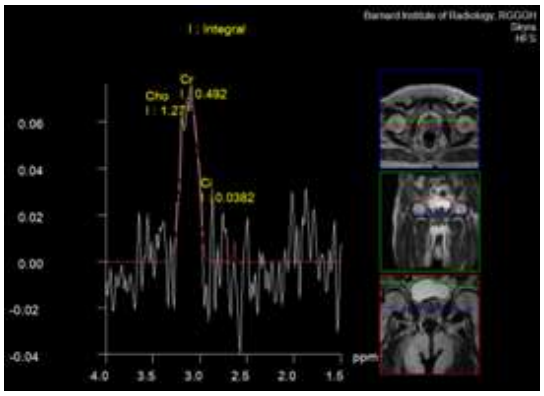

MR Spectroscopy

MRI Axial T2W, Diffusion, ADC images shows an well-defined circumscribed hypointense nodule in the peripheral zone of left mid gland of prostate.

On DWI, the nodule shows restricted diffusion with low ADC value on ADC map. ADC value: 0.751 x 10^{-3} mm^2/s. Dynamic contrast image shows heterogenous enhancement and Type II plateau pattern curve. MRS shows increased choline integral values.

CASE 3

Case of prostatic adenocarcinoma with Gleason score 9 (5+4) vs PI-RADS 3.

T2 Weighted

T2 Weighted

T2 Weighted

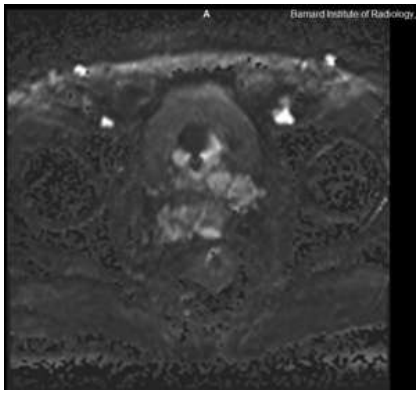

Diffusion Weighted

ADC

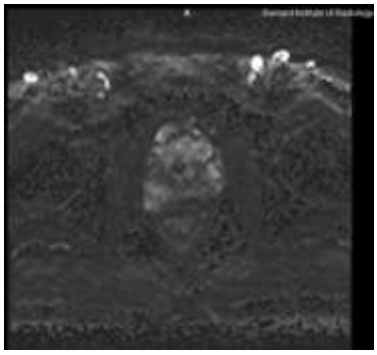

Diffusion Weighted

ADC

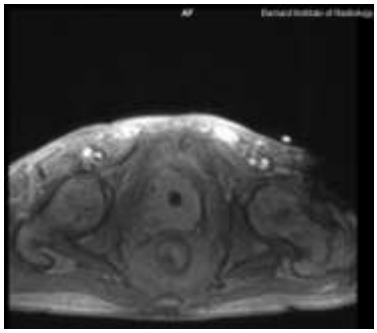

Post Contrast

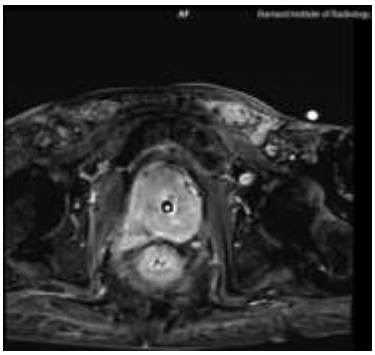

Subtracted

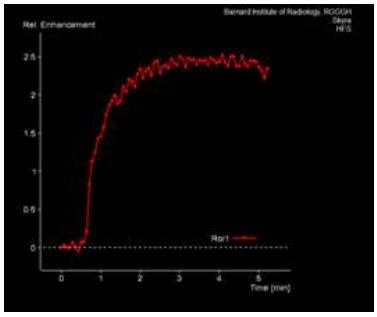

Time Intensity Curve

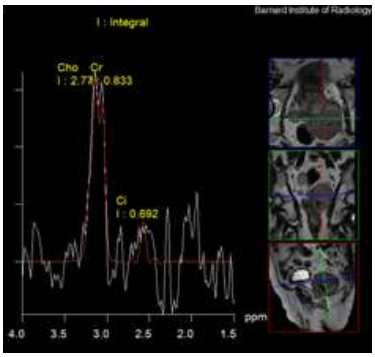

MR Spectroscopy

MRI Axial T2W, Diffusion, ADC images shows multiple, well- defined T2 hypointense nodules seen in the peripheral and transituion zone of base,apex and mid gland of prostate and shows bilateral seminal vesicle infiltration, extracapsular extension and neurovascular bundle infiltration.

On DWI, the nodule shows restricted diffusion with low ADC value on ADC map. ADC value: 0.58 x 10^{-3} mm^2/s. Dynamic contrast image shows homogenous enhancement and Type II plateau pattern curve on enhancement. MRS shows increased choline integral values.

CONCLUSION

Based on the findings of this study, it can be concluded that multi-parametric MRI PIRADS scoring in patients with raised PSA levels is an invaluable, non-invasive and feasible option to detect carcinoma prostate with a high sensitivity and specificity besides high predictive values and can help in identifying patients in need of biopsy and also helps in targeted biopsy and characterizing the extent and aggressiveness of the prostate cancer.

In summary, we confirm the hypothesis that there is a positive correlation between PI-RADS and Gleason's score i.e. significant increase in PI-RADS score with increase in Gleason's score and there is a significant negative correlation between mean tumor ADC value and Gleason's score. Thereby PI-RADS can noninvasively assess the aggressiveness of prostate cancer.

Also, the mean tumor ADC value could differentiate between low grade, intermediate grade and high grade tumors and can provide a useful adjunct to biopsy derived Gleason's score. This promising outcome of our study lead us to believe that incorporation of ADC values in multiparametric MRI could avoid surgery in patients with indolent tumor, for whom the potential risk of surgery outweighs the survival benefit.

BIBLIOGRAPHY

1) Jemal A, Siegel R, Xu J, Ward E. Cancer statistics, 2010. CA Cancer J Clin 2010; 60:277–300

2) Rais-Bahrami S, Siddiqui MM, Turkbey B, et al. Utility of multiparametric magnetic resonance imaging suspicion levels for detecting prostate cancer. J Urol 2013;190:1721–27

3) Djavan B, Ravery V, Zlotta A, et al. Prospective evaluation of prostate cancer detected on biopsies 1, 2, 3 and 4: when should we stop? J Urol 2001;166:1679–83.

4) Macura KJ. Multiparametric magnetic resonance imaging of the prostate: current status in prostate cancer detection, localization, and staging. Semin Roentgenol 2008;43:303–13.

5) Epstein JI, Allsbrook WC Jr, Amin MB, Egevad LL; ISUP Grading Committee. The 2005 International Society of Urological Pathology (ISUP) Consensus Conference on Gleason Grading of Prostatic Carcinoma. Am J Surg Pathol. 2005 Sep;29(9):1228-42.

6) Gleason DF, Mellinger GT. Prediction of prognosis for prostatic adenocarcinoma by combined histological grading and clinical staging. J Urol. 1974 Jan;111(1):58-64.

7) Bianco FJ Jr, Wood DP Jr, Cher ML, Powell IJ, Souza JW, Pontes JE. Ten-year survival after radical prostatectomy: specimen Gleason score is the predictor in organ-confined prostate cancer. Clin Prostate Cancer. 2003 Mar;1(4):242-7.

8) Rampersaud EN, Sun L, Moul JW, Madden J, Freedland SJ. Percent tumor involvement and risk of biochemical progression after radical prostatectomy. J Urol. 2008 Aug;180(2):571-6.

9) Kurhanewicz J, Vigneron DB, Males RG, Swanson MG, Yu K, Hricak H. The prostate: MR imaging and spectroscopy. Present and Future. Radiol Clin North Am 38:115-138, viii-ix, 2000.

10) B. Turkbey and P. L. Choyke, “Multiparametric MRI and prostate cancer diagnosis and risk stratification,” Current Opinion in Urology, vol. 22, no. 4, pp. 310–315, 2012

11) T. Penzkofer and C. M. Tempany-Afdhal, “Prostate cancer detection and diagnosis: the role of MR and its comparison with other diagnostic modalities-a radiologist’s perspective,” NMR in Biomedicine, vol. 27, no. 1, pp. 3–15, 2014

12) H. Zhou, R. R. Hallac, Q. Yuan et al., “Correlating multiparametric MRI with Gleason score in human prostate,” in International Society of Magnetic Resonance in Medicine Annual Conference, Milan, Itay,May 2014.

13) S. Verma, B. Turkbey, N. Muradyan et al., “Overview of dynamic contrast-enhanced MRI in prostate cancer diagnosis and management,” The American Journal of Roentgenology, vol. 198, no. 6, pp. 1277–1288, 2012.

14) Thompson J, Lawrentschuk N, Frydenberg M, Thompson L, Stricker P, USANZ. The role of magnetic resonance imaging in the diagnosis and management of prostate cancer. BJU Int 2013;112 (Suppl 2):6–20.

15) Gupta RT, Kauffman CR, Polascik TJ, Taneja SS, Rosenkrantz AB. The state of prostate MRI in 2013. Oncology (Williston Park) 2013;27:262– 70.

16) Le Bihan D, Breton E. Imagerie de diffusion in-vivo par résonance magnétique nucléaire. Comptes-Rendus de l'Académie des Sciences. 1985;93(5):27-34. Available from: <hal-00350090> (Accessed 12th December 2015).

17) Merboldt KD, Hanicke W, Frahm J. Self-diffusion NMR imaging using stimulated echoes. J Magn Reson (1969). 1985 Oct 1;64(3):479-86.

18) Taylor DG, Bushell MC. The spatial mapping of translational diffusion coefficients by the NMR imaging technique. Phys Med Biol. 1985 Apr;30(4):345-9.

19) Le Bihan D, Breton E, Lallemand D, Grenier P, Cabanis E, Laval-Jeantet M. MR imaging of intravoxel incoherent motions: application to diffusion and perfusion in neurologic disorders. Radiology. 1986 Nov;161(2):401-7.

20) Posse S, Cuenod CA, Le Bihan D. Human brain: proton diffusion MR spectroscopy. Radiology. 1993 Sep;188(3):719-25.

21) Sandrasegaran K, Tahir B, Patel A, Ramaswamy R, Bertrand K, Akisik FM, et al. The usefulness of diffusion-weighted imaging in the characterization of liver lesions in patients with cirrhosis. Clin Radiol. 2013 Jul;68(7):708-15.

22) Cappabianca S, Iaselli F, Reginelli A, D'Andrea A, Urraro F, Grassi R, et al. Value of diffusion-weighted magnetic resonance imaging in the characterization of complex adnexal masses. Tumori. 2013 Mar-Apr;99(2):210-7. doi: 10.1700/1283.14194.

23) Jensen JH, Helpern JA, Ramani A, Lu H, Kaczynski K. Diffusional kurtosis imaging: the quantification of non-gaussian water diffusion by means of magnetic resonance imaging. Magn Reson Med. 2005 Jun;53(6):1432-40.

24) Gibbs P, Pickles MD, Turnbull LW. Diffusion imaging of the prostate at 3.0 tesla. Invest Radiol. 2006 Feb;41(2):185-8.

25) Kim CK, Park BK, Han JJ, Kang TW, Lee HM. Diffusion-weighted imaging of the prostate at 3 T for differentiation of malignant and benign tissue in transition and peripheral zones: preliminary results. J Comput Assist Tomogr. 2007 May-Jun;31(3):449-54.

26) Pickles MD, Gibbs P, Sreenivas M, Turnbull LW. Diffusion-weighted imaging of normal and malignant prostate tissue at 3.0T. J Magn Reson Imaging. 2006 Feb;23(2):130-4.

27) Shimofusa R, Fujimoto H, Akamata H, Motoori K, Yamamoto S, Ueda T, et al. Diffusion-weighted imaging of prostate cancer. J Comput Assist Tomogr. 2005 Mar-Apr;29 (2):149-53.

28) Hosseinzadeh K, Schwarz SD. Endorectal diffusion-weighted imaging in prostate cancer to differentiate malignant and benign peripheral zone tissue. J Magn Reson Imaging. 2004 Oct;20(4):654-61.

29) Kim CK, Park BK, Kim B. High-b-value diffusion-weighted imaging at 3 T to detect prostate cancer: comparisons between b values of 1,000 and 2,000 s/mm2. AJR Am J Roentgenol. 2010 Jan;194(1):W33-7.

30) Kitajima K, Kaji Y, Kuroda K, Sugimura K. High b-value diffusion-weighted imaging in normal and malignant peripheral

zone tissue of the prostate: effect of signal-to-noise ratio. MagnReson Med Sci. 2008;7(2):93-9.

31) Sato C, Naganawa S, Nakamura T, Kumada H, Miura S, Takizawa O, et al. Differentiation of noncancerous tissue and cancer lesions by apparent diffusion coefficient values in transition and peripheral zones of the prostate. J Magn Reson Imaging. 2005 Mar;21(3):258-62.

32) Tamada T, Sone T, Jo Y, Toshimitsu S, Yamashita T, Yamamoto A, et al. Apparent diffusion coefficient values in peripheral and transition zones of the prostate: comparison between normal and malignant prostatic tissues and correlation with histologic grade. J Magn Reson Imaging. 2008 Sep;28(3):720-6.

33) Tanimoto A, Nakashima J, Kohno H, Shinmoto H, Kuribayashi S. Prostate cancer screening: the clinical value of diffusion-weighted imaging and dynamic MR imaging in combination with T2-weighted imaging. J Magn Reson Imaging. 2007 Jan;25(1):146-52.

34) desouza NM, Reinsberg SA, Scurr ED, Brewster JM, Payne GS. Magnetic resonance imaging in prostate cancer: the value of apparent diffusion coefficients for identifying malignant nodules. Br J Radiol. 2007 Feb;80(950):90-5.

35) Kumar V, Jagannathan NR, Kumar R, Das SC, Jindal L, Thulkar S, et al. Correlation between metabolite ratios and ADC values of prostate in men with increased PSA level. Magn Reson Imaging. 2006 Jun;24(5):541-8.

36) Cooper JF, and Imfeld H. The role of citric acid in the physiology of the prostate: A preliminary report. J Urol 81:157-163, 1959.

37) Cooper JF, and Farid I. The role of citric acid I the physiology of the prostate: Lactic/citrate rations in benign and malignant prostatic homogenates as an index of prostatic malignancy. J Urol 92:533-536, 1964.

38) Costello LC, Liu Y, Franklin RB, Kennedy MC. Zinc inhibition of mitochondrial aconitase and its importance in citrate metabolism of prostate epithelial cells. J Biol Chem 46(14):28875-81, 1997.

39) Costello LC and Franklin RB. Novel role of zinc in the regulation of prostate citrate metabolism and its implications in prostate cancer. The Prostate 35:285-296, 1998.

40) Zaichick VY, Sviridova TV, Zaichick SV. Zinc concentration in human prostatic fluid: Normal, chronic prostatitis, adenoma and cancer. Int Urol Nephrol 28:687-694, 1996.

41) Zaichick VY, Sviridova TV, Zaichick SV. Zinc in the human prostate gland: Normal hyperplasia, cancerous. Int Urol Nephrol 29:565-574, 1997.

42) Costello LC, Franklin RB, Liu Y, Kennedy MC. Zinc causes a shift toward citrate at equilibrium of the m-aconitase reaction of prostate mitochondria. Inorg Biochem 78:161-165, 2000.

43) Hricak H, White S, Vigneron D, et al. Carcinoma of the prostate gland: MR imaging with pelvic phased-array coils versus integrated endorectal-pelvic phased-array coils. Radiology 193:703-709, 1991.

44) Kurhanewicz J, Vigneron DB, Males RG, Swanson MG, Yu K, Hricak H. The prostate: MR imaging and spectroscopy. Present and Future. Radiol Clin North Am 38:115-138, viii-ix, 2000.

45) Perrotti M, Han KR, Epstein RE, Kennedy EC, Rabbani F, Badani K, Pantuck AJ, Weiss RE, Cummings KB. Prospective evaluation of endorectal magnetic resonance imaging to detect tumor foci in men with prior negative prostatic biopsy: a pilot study. J Urol 162(4) 1314-7, 1999.

46) Torricelli P, Iadanza M, De Santis M, Pollastri CA, Cesinaro AM, Trentini G, Romagnoli R. Magnetic resonance with endorectal coil in the local staging of prostatic carcinoma. Comparison with

histologic macrosectionis in 40 cases. Radiol Med (Torino) 97(6):491-498, 1999.

47) Negendank W. Studies of human tumors by MRS: a review. NMR Biomed 5(5):303-324, 1992.

48) Costello LC and Franklin RB. Bioenergetic theory of prostate malignancy. Prostate 25(3):162- 166, 1994.

49) Costello LC, Franklin RB, and Narayan P. Citrate in the diagnosis of Prostate Cancer. The Prostate 38:237-245, 1999.

50) Cornel EB, Smuts GA, Oosterhof GO, et al. Characterization of human prostate cancer, benign prostatic hyperplasia and normal prostate by in vitro 1H and 31P magnetic resonance spectroscopy. J Urol 150:2019-24, 1993.

51) Kurhanewicz J, Thomas A, Jajodia P. et al., 31P spectroscopy of the human prostate gland in vivo using a transrectal probe. Magn Reson Med 22:404-413, 1991.

52) Kurhanewicz J, Dahiya R, Macdonald JM et al. Phosphorus metabolite characterization of human prostatic adenocarcinoma in a nude mouse model by 31P magnetic resonance spectroscopy and high pressure liquid chromatography. NMR Biomed 5:185-192, 1992.

53) Schiebler M, Miyamoto KK, White M, Maygarden SJ, Mohler JL. In vitro high resolution 1Hspectroscopy of the human prostate: benign prostatic hyperplasia, normal peripheral zone and adenocarcinoma. Magn Reson Med 29:285-291, 1993.

54) Kurhanewicz J, Dahiya R, Macdonald JM, Chang LH, James TL, Narayan P. Citrate alterations in primary and metastasis human prostatic Aden carcinomas: 1H magnetic resonance spectroscopy and biochemical study. Magn Reson Med 29:149-157, 1993.

55) Van der Graaf M, Schipper RG, Oosterhof GO, Schalken JA, Verhofstad AA, Heerschap A. Proton MR spectroscopy of prostatic tissue focused on the detection of spermine, a possible biomarker of malignant behavior in prostate cancer. Magma 10:153-159, 2000.

56) Childs AC, Mehta DJ, Gerner EW. Polyamine-dependent gene expression. Cell Mol Life Sci 60:1394-406, 2003.

57) Babban N and Gerner EW. Polyamines as modifiers of genetic risk factors in human intestinal cancers. Biochem. Soc Trans. 31:388-392, 2003.

58) Frahm J, Bruhn H, Gyngell ML, Merbolt KD, Hanicke W, Sauter R. Localized high-resolution proton NMR spectroscopy using

echoes: initial applications to human brain in vivo. Magn Reson Med 9:79-93, 1989.

59) Bottomley PA. Spatial localization in NMR spectroscopy in vivo. Ann N Y Acad Sci, 508:333-348, 1987.

60) Heerschap A, Jager G, de Koster A, Barentsz J, de la Rosette J, Debruyne F and Ruijs J. 1H MRS of prostate pathology, in Proceedings of Soc of Magn Reson Med , 12th annual meeting, New York, 1993, p213.

61) Kurhanewicz J, Vigneron DB, Nelson SJ, Hricak HJ, McDonald JM, Konety B, Narayana P. Citrate as an in vivo marker to discriminate prostate cancer from benign hyperplasia and normal prostate peripheral zone: detection via localized proton spectroscopy. Urology 45:459-66, 1995.

62) Brown TR. Practical applications of chemical shift imaging. NMR Biomed. 5:238-243, 1992.

63) Brown TR, Kincaid BM, and Ugurbil K. NMR chemical shift in three dimensions. Proc Natl Acad Sci USA, 79:3523-26, 1982.

64) Maudsley AA, Hilal SK, Simon HE, Wittekoek S. In vivo MR spectroscopic imaging. Work in progress. Radiology153:745-750m 1984.

65) Luyten PR, Marien AJ, den HJ. Acquisition and quantitation in proton spectroscopy. NMR Biomed 4:64-69, 1991.

66) Star-Lack J, Nelson SJ, Kurhanewicz J, Huang LR, Vigneron DB. Improved water and lipid suppression for 3D PRESS CSI using RF Band selective inversion with gradient dephasing (BASING). Magn Reson Med 38:311-321, 1997.

67) Tran T-KC, Vigneron DB, Sailasuta N, Tropp J, Le Roux P, Kurhanewicz J, Nelson S, Hurd R. Very selective suppression pulses for clinical MRSI studies of brain and prostate cancer. Magn Reson Medi 43:23-33, 2000.

68) Star-Lack J, Vigneron DB, Pauly J, Kurhanewicz J, Nelson SJ. Improved solvent suppression and increased spatial excitation bandwidths for three-dimensional PRESS CSI using phase compensating spectral/spatial spin-echo pulses. J Magn Reson Imaging 7:745-757,1997.

69) Males RG, Vigneron DB, Star-Lack J, Falbo SC, Nelson SJ, Hricak H, Kurhanewicz J. Clincal application of BASING and Spectral/Spatial Water and Lipid Suppression Pulses for Prostate Cancer Staging and Localization by In Vivo 3D 1H Magnetic

Resonance Spectroscopic Imaging. Magn Reson Med 43:17-22, 2000.

70) Kurhanewicz J, Vigneron DB, Hricak H, Narayan P, Carroll P, Nelson SJ. Three-dimensional H-1 MR spectroscopic imaging of the in Situ human prostate with high (0.24-0.7 cm3) spatial resolution. Radiology 198:795-805, 1996.

71) Yu KK, Scheidler J, Hricak H, Vigneron DB, Zaloudek CJ, Males RG, Nelson SJ, Carroll PR, Kurhanewicz J. Prostate Cancer: Prediction of extracapsular extension with endorectal MR imaging and three-dimensional proton MR spectroscopic imaging. Radiology 213:481-88, 1999.

72) Coakley FV, Kurhanewicz J, Liu Y et al. Prostate cancer tumor volume: Measurement by endorectal MR imaging and MR spectroscopic imaging. Radiology 223:91-97, 2002.

73) Wefer AE, Hricak H, Vigneron DB, et al. Sextant localization of prostate cancer: comparison of sextant biopsy, magnetic resonance imaging and magnetic resonance spectroscopic imaging with step section histology. J Urol 164:400-404, 2000.

74) Kurhanewicz J, Vigneron DB, Nelson SJ. Three-dimensional magnetic resonance spectroscopic imaging of brain and prostate cancer. Neoplasia 2:166-189, 2000.

75) Scheenen TWJ, Klomp DWJ, Roll SA, Futterer JJ, Barentsz JO, Heerschap A. Fast acquisitionweighted three-dimensional proton MR spectroscopic imaging of the human prostate. Magn Reson Med 52:80-88, 2004.

76) Scheenen TWJ, Gambarota G, Weiland E, Klomp DWJ, Futterer JJ, Barentsz, Heerschap A. Optimal timing for in vivo 1H-MR Spectroscopic imaging of the human prostate at 3T. MagnReson Med 53:1268-74, 2005.

77) Scheenen T, Weiland E, Futterer J, van Hecke P, Bachert P, Villeirs G, Lu J, Lichy M, Holshouser B, Roell S, Barentsz J, Heerschap A. Preliminary results of IMAPS: An International Multi-Centre Assessment of Prostate MR Spectroscopy. Proceedings of the Thirteenth Int Soc Mag Reson Med., Miami Beach, 2005, p 260.

78) Jung JA, Coakley FV, Vigneron DB, Swanson MG, Qayyum A, Weinberg V, Jones KD, Carroll PR, Kurhanewicz J. Prostate depiction at endorectal MR spectroscopic imaging: Investigation

of a standardized evaluation system. Radiology 233:701-708, 2004.

79) Swanson MG, Vigneron DB, Tran T-K C, Kurhanewicz J. Magnetic resonance imaging and spectroscopic imaging of prostate cancer. Cancer Investigation 19(5):510-523, 2001.

80) Hricak H. MR imaging and MR spectroscopic imaging in the pre-treatment evaluation of prostate cancer. Br J Radiol 78:S103-S111, 2005.

81) D'Amico AV, Whittington R, Malkowicz B, et al. Endorectal magnetic resonance imaging as a predictor of biochemical outcome after radical prostatectomy in men with clinically localized prostate cancer. J Urol 164:759-763, 2000.

82) DiBiase SJ, Hosseinzadeh K, Gullapalli RP, et al. Magnetic resonance spectroscopic imagingguided brachytherapy for localized prostate cancer. Int J Radiat Oncol Biol Phys 52L429-8, 2002.

83) Mizowaki T, Cohen GN, Fung AY, Zaider M. Towards integrating functional imaging in the treatment of prostate cancer with radiation: the registration of the MR spectroscopy to ultrasound/CT images and its implementation in treatment planning. Int J Radiat Oncol Biol Phys 54:1558-64, 2002.

84) Sosna J, Rofsky NM, Gaston SM, DeWolf WC, Lenkinski RE. Determinations of prostate volume at 3-Tesla using an external phased array coil: Comparison to pathologic specimens. Acad Radiol 10:846-853, 2003.

85) Sosna J, Pedrosa I, Dewolf WC, Mahallati H, Lenkinski RE, Rofsky NM. MR imaging of the prostate at 3 Tesla: Comparison of an external phased-array coil to imaging with an endorectal coil at 1.5 Tesla. Acad Radiol 11:857-862, 2004.

86) Bloch BN, Rofsky NM, Baroni RH, Marquis RP, Pedrosa I, Lenkinski RE. 3 Tesla magnetic resonance imaging of the prostate with combined pelvic phased-array and endorectal coils: Initial experience. Acad Radiol 11:863-867, 2004.

87) Wantanabe et al.,1968.Wantanabe H, Kato H, Kato T, Masayoshi M: Diagnostic applications of the ultrosonotomography for the prostate. Jpn J Urol 1968; 59:273-279.

88) Hodge et al., 1989a. Hodge KK, Mc Neal JE, Stamey TA: Ultrasound guided transrectal core biopsies of the palpably abnormal prostate. J Urol 1989; 142:66-70.

89) Hodge et al., 1989b. Hodge KK, Mc Neal JE, Terris MK, Stamey TA: Random systematic versus directed ultrasound guided transrectal core biopsies of the prostate. J Urol 1989;142:71-75.

90) Halpern and strup.2000. Halpern EJ, Strup SE: Using grey scale and color and power Doppler sonography to detect prostatic cancer. AJR 2000; 174:623-627.

91) Beerlage, 2003. Beerlage HP: Alternative therapies for localized prostate cancer. Curr Urol Rep 2003; 4: 216-220.

92) Shinohara et al.,1989. Shinohara K, Wheeler TM, Scardino PT: The appearance of prostate cancer on transrectal ultrasonography: Correlation of imaging and pathological examinations. J Urol 1989; 142:76-82.

93) Onur et al.,2004. Onur R, Littrup PJ, Pontes JE, Biancojr FJ: Contemporary impact of trans rectal ultrasound lesion for prostate cancer detection. J Urol 2004; 172: 512-514.

94) Bude and Rubin, 1996. Bude RO, Rubin JM: Power Doppler sonography. Radiology 1996; 200: 21-23.

95) Klauser et al., 2003. KLAUSER a, Koppel staetter F, Horninger W, et al: Real-time elastography for prostate cancer detection: Preliminary experience [abstract] Radio Soc North Am 2003; 89-665-666.

96) Ives et al.,2005. Ives EP, Waldman L, Gomella LG, Halpern EJ: Proceeding of the 105 th Annual meeting of the American Roentgen Ray Socity. AJR Am J Roentgenol 2005;[4 suppl]: 61.

97) Prando A. Diffusion-weighted MRI of peripheral zone prostate cancer: comparison of tumor apparent diffusion coefficient with Gleason score and percentage of tumor on core biopsy. International braz j urol. 2010 Aug;36(4):504-17.

98) Fehr D, Veeraraghavan H, Wibmer A, Gondo T, Matsumoto K, Vargas HA, Sala E, Hricak H, Deasy JO. Automatic classification of prostate cancer Gleason scores from multiparametric magnetic resonance images. Proceedings of the National Academy of Sciences. 2015 Nov 17;112(46):E6265-73.

99) Ouzzane A, Puech P, Lemaitre L, Leroy X, Nevoux P, Betrouni N, Haber GP, Villers A. Combined multiparametric MRI and targeted biopsies improve anterior prostate cancer detection, staging, and grading. Urology. 2011 Dec 31;78(6):1356-62.

100) Delongchamps NB, Beuvon F, Eiss D, Flam T, Muradyan N, Zerbib M, Peyromaure M, Cornud F. Multiparametric MRI is helpful to predict tumor focality, stage, and size in patients diagnosed with unilateral low-risk prostate cancer. Prostate cancer and prostatic diseases. 2011 Sep 1;14(3):232-7.

101) de Rooij M, Hamoen EH, Fütterer JJ, Barentsz JO, Rovers MM. Accuracy of multiparametric MRI for prostate cancer detection: a

meta-analysis. American Journal of Roentgenology. 2014 Feb; 202(2):343-51.

102) Citak-Er F, Vural M, Acar O, Esen T, Onay A, Ozturk-Isik E. Final Gleason Score Prediction Using Discriminant Analysis and Support Vector Machine Based on Preoperative Multiparametric MR Imaging of Prostate Cancer at 3T. BioMed research international. 2014 Dec 2; 2014.

103) Arsov C, Becker N, Rabenalt R, Hiester A, Quentin M, Dietzel F, Antoch G, Gabbert HE, Albers P, Schimmöller L. The use of targeted MR-guided prostate biopsy reduces the risk of Gleason upgrading on radical prostatectomy. Journal of cancer research and clinical oncology. 2015 Nov 1;141(11):2061-8.

104) Siddiqui MM, Rais-Bahrami S, Truong H, Stamatakis L, Vourganti S, Nix J, Hoang AN, Walton-Diaz A, Shuch B, Weintraub M, Kruecker J. Magnetic resonance imaging/ultrasound–fusion biopsy significantly upgrades prostate cancer versus systematic 12-core transrectal ultrasound biopsy. European urology. 2013 Nov 30;64(5):713-9.

105) Hambrock T, Hoeks C, Hulsbergen-Van de Kaa C, Scheenen T, Fütterer J, Bouwense S, van Oort I, Schröder F, Huisman H, Barentsz J. Prospective assessment of prostate cancer

aggressiveness using 3-T diffusion-weighted magnetic resonance imaging–guided biopsies versus a systematic 10-core transrectal ultrasound prostate biopsy cohort. European urology. 2012 Jan 31;61(1):177-84.

106) Mowatt G, Scotland G, Boachie C, Cruickshank M, Ford JA, Fraser C, Kurban L, Lam TB, Padhani AR, Royle J, Scheenen TW. The diagnostic accuracy and cost-effectiveness of magnetic resonance spectroscopy and enhanced magnetic resonance imaging techniques in aiding the localisation of prostate abnormalities for biopsy: a systematic review and economic evaluation. Health Technology Assessment. 2013.

107) Schoots IG, Roobol MJ, Nieboer D, Bangma CH, Steyerberg EW, Hunink MM. Magnetic resonance imaging–targeted biopsy may enhance the diagnostic accuracy of significant prostate cancer detection compared to standard transrectal ultrasound-guided biopsy: a systematic review and meta-analysis. European urology. 2015 Sep 30;68(3):438-50.

108) Tonttila PP, Lantto J, Pääkkö E, Piippo U, Kauppila S, Lammentausta E, Ohtonen P, Vaarala MH. Prebiopsy multiparametric magnetic resonance imaging for prostate cancer diagnosis in biopsy-naive men with suspected prostate cancer based on elevated prostate-specific antigen values: results from a

randomized prospective blinded controlled trial. European urology. 2015 May 29.

109) Kumar V, Jagannathan NR, Kumar R, Thulkar S, Gupta SD, Dwivedi SN, et al. Apparent diffusion coefficient of the prostate in men prior to biopsy: determination of a cut-off value to predict malignancy of the peripheral zone. NMR Biomed. 2007 Aug;20(5):505-11.

110) Nagayama M, Watanabe Y, Terai A, Araki T, Notohara K, Okumura A, et al. Determination of the cutoff level of apparent diffusion coefficient values for detection of prostate cancer. Jpn J Radiol. 2011 Aug;29(7):488-94. doi: 10.1007/s11604-011-0586-6. Epub 2011 Sep 1.

111) Kingsley PB, Monahan WG. Selection of the optimum b factor for diffusion-weighted magnetic resonance imaging assessment of ischemic stroke. Magn Reson Med. 2004 May;51(5):996-1001.

112) Hambrock T, Somford DM, Huisman HJ, van Oort IM, Witjes JA, Hulsbergen-van de Kaa CA, et al. Relationship between apparent diffusion coefficients at 3.0-T MR imaging and Gleason grade in peripheral zone prostate cancer. Radiology. 2011 May;259(2):453-61.

113) Kim JH, Kim JK, Park BW, Kim N, Cho KS. Apparent diffusion coefficient: prostate cancer versus noncancerous tissue according to anatomical region. J Magn Reson Imaging. 2008 Nov;28(5):1173-9.

114) Yoshimitsu K, Kiyoshima K, Irie H, Tajima T, Asayama Y, Hirakawa M, et al. Usefulness of apparent diffusion coefficient map in diagnosing prostate carcinoma: correlation with stepwise histopathology. J Magn Reson Imaging. 2008 Jan;27(1):132-9.

115) Verma S, Rajesh A, Morales H, Lemen L, Bills G, Delworth M, et al. Assessment of aggressiveness of prostate cancer: correlation of apparent diffusion coefficient with histologic grade after radical prostatectomy. AJR Am J Roentgenol. 2011 Feb;196(2):374-81.

116) Woodfield CA, Tung GA, Grand DJ, Pezzullo JA, Machan JT, Renzulli JF 2nd. Diffusion-weighted MRI of peripheral zone prostate cancer: comparison of tumor apparent diffusion coefficient with Gleason score and percentage of tumor on core biopsy. AJR Am J Roentgenol. 2010 Apr;194(4):W316-22.

117) Yağci AB, Ozari N, Aybek Z, Düzcan E. The value of diffusion-weighted MRI for prostate cancer detection and localization. Diagn Interv Radiol. 2011 Jun;17(2):130-4. doi: 10.4261/1305-3825.DIR.3399-10.1. Epub 2010 Aug 6.

118) Luczyńska E, Heinze-Paluchowska S, Domalik A, Cwierz A, Kasperkiewicz H, Blecharz P, et al. The Utility of Diffusion Weighted Imaging (DWI) Using Apparent Diffusion Coefficient (ADC) Values in Discriminating Between Prostate Cancer and Normal Tissue. Pol J Radiol. 2014 Dec 2;79:450-5. doi: 10.12659/PJR.890805. eCollection 2014.

119) Anwar SS, Anwar Khan Z, Shoaib Hamid R, Haroon F, Sayani R, Beg M, et al. Assessment of apparent diffusion coefficient values as predictor of aggressiveness in peripheral zone prostate cancer: comparison with Gleason score. ISRN Radiol. 2014 Feb 9;2014:263417. doi: 10.1155/2014/263417. eCollection 2014.

120) De Cobelli F, Ravelli S, Esposito A, Giganti F, Gallina A, Montorsi F, et al. Apparent diffusion coefficient value and ratio as noninvasive potential biomarkers to predict prostate cancer grading: comparison with prostate biopsy and radical prostatectomy specimen. AJR Am J Roentgenol. 2015 Mar;204(3):550-7.

121) Hoeks CM, Barentsz JO, Hambrock T, Yakar D, Somford DM, Heijmink SW, Scheenen TW, Vos PC, Huisman H, van Oort IM, Witjes JA. Prostate cancer: multiparametric MR imaging for

detection, localization, and staging. Radiology. 2011 Oct;261(1):46-66.

122) Hegde JV, Mulkern RV, Panych LP, Fennessy FM, Fedorov A, Maier SE, Tempany C. Multiparametric MRI of prostate cancer: An update on state‐of‐the‐art techniques and their performance in detecting and localizing prostate cancer. Journal of Magnetic Resonance Imaging. 2013 May 1;37(5):1035-54.

123) Freedland SJ, Kane CJ, Amling CL, Aronson WJ, Terris MK, Presti JC Jr; SEARCH Database Study Group. Upgrading and downgrading of prostate needle biopsy specimens: risk factors and clinical implications. Urology. 2007 Mar;69(3):495-9.

124) Mazaheri Y, Hricak H, Fine SW, Akin O, Shukla-Dave A, Ishill NM, et al. Prostate tumor volume measurement with combined T2-weighted imaging and diffusion-weighted MR: correlation with pathologic tumor volume. Radiology. 2009 Aug;252(2):449-57.

125) Zelhof B, Pickles M, Liney G, Gibbs P, Rodrigues G, Kraus S, et al. Correlation of diffusion-weighted magnetic resonance data with cellularity in prostate cancer. BJU Int. 2009 Apr;103(7):883-8.

126) Vander cruijsen-Koeter et al., 2001. Vander cruijsen-Koeter IW, Wildhagen MF, Dekoneis HJ, Schroder FH: The value of current

diagnostic tests in prostate cancer screening. BJU int 2001; 88: 458.

127) Carter et al., 1989. Carter HB, Hamper UM, Sheth S, et al: Evaluation of transrectal ultrasound in the diagnosis of prostate cancer. J Urol 1989: 142: 1008.

128) Ellis et al., 1994. Ellis WJ, Chetner MP, Preston SD, Brawer MK: Diagnosis of prostatic carcinoma: The yield of serum prostate specific antigen, digital rectal examination and transrectal ultrasonography. J Urol 1994; 52: 1520

129) Carter, 2000. Carter HB, A PSA threshold of 4ng/ml for early detection of prostate cancer. The only rational approach for men 50 years old and older. Urology 2000: 55: 796

130) Carter, 2004. Carter HB; Prostate cancer in men with low PSA levels- Must we find them ? N Engl J Med 2004; 350: 2292

131) Catalona et al., 2000a. Catalona WJ, Ramos CG, Carvalhal GF, Yan Y: Lowering PSA cutoffs to enhance detection of curable prostate cancer. Urology 2000; 55: 791.

132) Flanigan et al., 1994. Flanigan RC, Catalona WJ, Richie JP, et al: Accuracy of digital rectal examination and transrectal ultrasonography in localizing prostate cancer. J Urol 1994; 152: 1506.

133) Rifkin et al., 1990. Rifkin MD, Zerhowni EA, Gatsonis CA, et al: Comparison of magnetic resonance imaging and ultrasonography in staging early prostate cancer. Results of a multi institutional co operative trial. N Engl J Med 1990; 323: 621.

134) Naughton CK, Smith DS, Humphrey PA, Catalona WJ, Keetch DW. Clinical and pathological tumour characterics of prostate cancer as a function of number of biopsy cores: A retrospective study. Urology 1998; 52: 808-13.

135) Rabbani F, Stroumbakis N, Kava BR, Cookson MS, Fair WR. Incidence and clinical significance of false negative sectant prostate biopsies. J Urol 1998; 159: 1247-50

136) Kumar V, Jagannathan NR, Kumar R, et al. Transrectal ultrasound guided biopsy of prostate voxels identified as suspicious of malignancy on three dimensional 1H MR Spectroscopic imaging in patients with abnormal digital rectal examination or raised prostate specific antigen level of 4-10ng/ml. NMR Biomed 2007; 20: 11-20

137) Kumar V, Jagannathan NR, Kumar R et al., 3D 1H MRI based TRUS guided biopsies in men with suspected prostate cancer. Proc inti soc Mag Reson Med 2006: 14: 1790.

ABBREVIATIONS

ADC	Apparent Diffusion Co-efficient
ANOVA	Analysis Of Variance
cm	centimeter
CZ	Central zone
DCE-MRI	Dynamic Contrast Enhanced Magnetic Resonance Imaging
DW-MRI	Diffusion Weighted Magnetic Resonance Imaging
DWI	Diffusion Weighted Imaging
DRE	Digital Rectal Examination
ECE	Extracapsular extension
EPI	Echo Planar Imaging
FLAIR	Fluid Attenuation Inversion Recovery
FOV	Field Of View
FSE	Fast Spin Echo
GS	Gleason's score
LN	Lymphnodes
mm	millimeter
MRI	Magnetic Resonance Imaging
MRS	Magnetic Resonance Spectroscopy
NPV	Negative Predictive Value
NVBI	Neurovascularbundle involvement
PPV	Positive Predictive Value
PSA	Prostate specific antigen
PIRADS	Prostate Imaging - Reporting and Data system

PZ	Peripheral zone
ROI	Region of Interest
ROC	Receiver Operating Characteristic Curve
s	seconds
SD	Standard Deviation
SNR	Signal to Noise Ratio
sPSA	serum Prostate Specific Antigen
SPSS	Statistical Package for the Social Sciences
SVI	Seminal vesicle invasion
T2WI	T2 Weighted Imaging
TE	Time to Echo
TR	Time to Relax
TNM	Tumor, Nodes and Metastases
TRUS	Trans-rectal Ultrasound
TZ	Transition zone

PROFORMA FOR MP MR STUDY OF CA PROSTATE

STUDY TITLE:

"ANALYSIS OF MULTIPARAMETRIC MRI DATA IN PROSTATIC CARCINOMA – PIRADS & CORRELATION WITH GLEASON SCORE"

Sl. No:

Name:

Age/Sex:

Occupation:

Address:

Presenting Complaints and History:

INVESTIGATIONS :

Ultrasound findings:

Transabdominal USG:

Transrectal USG:

Biopsy Done or not:

Serum PSA-

Radionucleide scan Done or not:

T2 WEIGHTED IMAGE	
ADC	
MRS - Choline + creatinine / citrate ratio	
DYNAMIC CONTRAST MR	
HPE (GLEASONS SCORE)	
PI-RADS SCORE	

PATIENT INFORMATION SHEET

“ANALYSIS OF MULTIPARAMETRIC MRI DATA IN PROSTATIC CARCINOMA – PIRADS AND CORRELATION WITH GLEASON SCORE’’

- Your cooperation would be valuable to us for the same

- The privacy of patients in the research will be maintained throughout the study. In the event of any publication or presentation resulting from the research, no personally identifiable information will be shared.

- Taking part of the study is voluntary.you are free to decide whether to participate in this study or to withdraw at any time.your decision will not result in any loss of benefits to which your are otherwise entitled.

- The result of the special study may be intimated to you at the end of the study period or during the study if anything is found abnormal which may aid in the management or treatment.

Signature of the investigator Signature of participant

G.SAKTHIVEL RAJA

Date:

PATIENT CONSENT FORM

STUDY TITLE:

"ANALYSIS OF MULTIPARAMETRIC MRI DATA IN PROSTATIC CARCINOMA – PIRADS AND CORRELATION WITH GLEASON SCORE''

PARTICIPANT NAME :

Age: Sex: IP.NO. :

I confirm that I have understood the purpose of procedure for the above study. I have the opportunity to ask the questions and all my questions and doubts have been answered to my satisfaction.

I have been explained about the pitfall in the procedure. I have been explained about the safety , advantage and disadvantage of the technique.

I understand that my participation in the study is voluntary and that I'm free to withdraw at anytime without giving any reason.

I understand that investigator, regulatory authorities and the ethics committee will not need my permission to look at my health records both in respect to current study and any further research that may be conducted in relation to it , even if I withdraw from the study.

I understand that my identity will not be revealed in any information released to third parties or published, unless as required under the law. I agree not to restrict the use of any data or results that arise from the study.

I HEREBY CONSENT TO UNDERGO COMPLETE PHYSICAL EXAMINATION, BIOCHEMICAL AND RADIOLOGICAL INVESTIGATION ERTAINING TO THE STUDY.

Signature/Thumb Impression of Participant

INSTITUTIONAL ETHICS COMMITTEE
MADRAS MEDICAL COLLEGE, CHENNAI 600 003

EC Reg.No.ECR/270/Inst./TN/2013
Telephone No.044 25305301A
Fax: 011 25363970

CERTIFICATE OF APPROVAL

To
Dr.G.Sakthivelraja
II Year Post Graduate in M.D.Radio Diagnosis
Madras Medical College
Chennai

Dear Dr.G.Sakthivelraja,

The Institutional Ethics Committee has considered your request and approved your study titled **"ANALYSIS OF MULTIPARAMETRIC MRI DATA IN PROSTATIC CARCINOMA – PIRADS AND CORRELATION WITH GLEASON SCORE " NO. 17012017.**

The following members of Ethics Committee were present in the meeting hold on **03.01.2017** conducted at Madras Medical College, Chennai 3

1.Dr.C.Rajendran, MD.,	:Chairperson
2.Dr.M.K.Muralidharan,MS.,M.Ch.,Dean, MMC,Ch-3	:Deputy Chairperson
3.Prof.Sudha Seshayyan,MD., Vice Principal,MMC,Ch-3	: Member Secretary
4.Prof.B.Vasanthi,MD., Prof.of Pharmacology.,MMC,Ch-3	: Member
5.Prof.A.Rajendran,MS, Prof. of Surgery,MMC,Ch-3	: Member
6.Prof.N.Gopalakrishnan,MD,Director,Inst.of Nephrology,MMC,Ch	: Member
7.Prof.Baby Vasumathi,MD.,Director, Inst. of O & G	: Member
8.Prof.K.Ramadevi,MD.,Director,Inst.of Bio-Che,MMC,Ch-3	: Member
9.Prof.R.Padmavathy, MD, Director,Inst.of Pathology,MMC,Ch-3	: Member
10.Prof.S.Mayilvahanan,MD,Director, Inst. of Int.Med,MMC, Ch-3	: Member
11.Tmt.J.Rajalakshmi, JAO,MMC, Ch-3	: Lay Person
12.Thiru S.Govindasamy, BA.,BL.,High Court,Chennai	: Lawyer
13.Tmt.Arnold Saulina, MA.,MSW.,	:Social Scientist

We approve the proposal to be conducted in its presented form.

The Institutional Ethics Committee expects to be informed about the progress of the study and SAE occurring in the course of the study, any changes in the protocol and patients information/informed consent and asks to be provided a copy of the final report.

Member Secretary – Ethics Committee

MEMBER SECRETARY
INSTITUTIONAL ETHICS COMMITTEE

PLAGIARISM CERTIFICATE

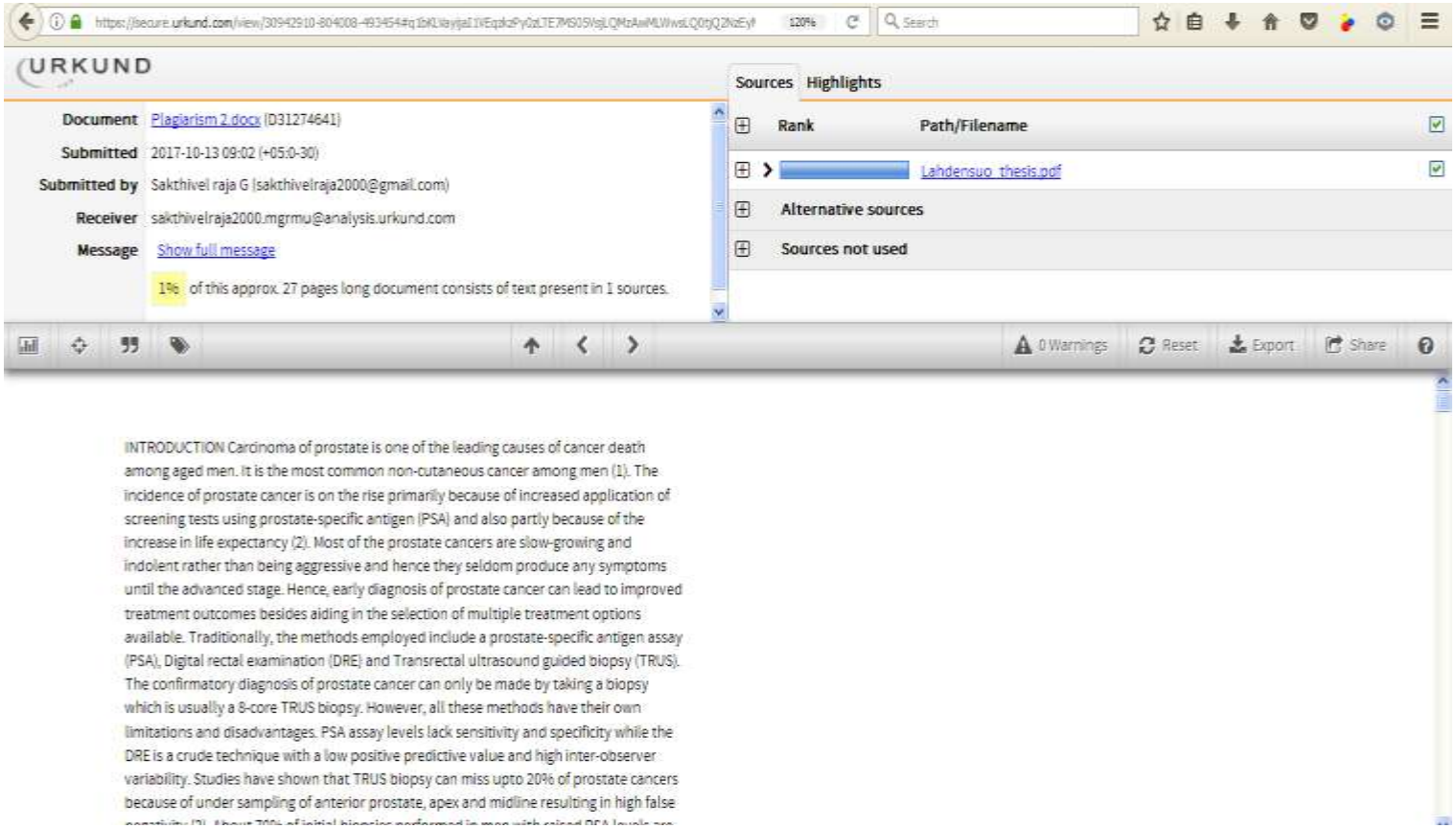

URKUND

Urkund Analysis Result

Analysed Document: Plagiarism 2.docx (D31274641)
Submitted: 10/13/2017 5:32:00 AM
Submitted By: sakthivelraja2000@gmail.com
Significance: 1 %

Sources included in the report:

Lahdensuo_thesis.pdf (D27277567)

Instances where selected sources appear:

1

PLAGIARISM CERTIFICATE

This is to certify that this dissertation work titled "ANALYSIS OF MULTIPARAMETRIC MRI DATA IN PROSTATIC CARCINOMA- PI-RADS AND CORRELATION WITH GLEASON SCORE IN A 3T MRI" of the candidate Dr.G.SAKTHIVEL RAJA with Registration Number 201518003 for the award of M.D RADIODIAGNOSIS. I personally verified the urkund.com website for plagiarism check. I found that the uploaded file containing from introduction to conclusion pages shows a result of 1% plagiarism in this dissertation.

Guide and supervisor sign with seal

S.NO.	NAME	AGE	TRUS PROSTATE VOLUME	PSA(ng/ml)	T2 W								DIFF/ ADC	MRS		DCE	PI-RADS T2W+DWI+ DCE	GLEASON"S SCORE
					FOCAL				SVI	ECE	NVBI	LN		CHOLINE	CITRATE			
					PZ	TZ+CZ	PZ	TZ+CZ										
1	RAJAMANICKAM	66	35	71.8			p		N	N	N	N	0.87	I	D	P	3	6(3+3)
2	ABDUL KUTHOSS	75	48	100	P				P		P	P	0.74	I	D	P	4	7(3+4)
3	DHATCHANAMOORTHY	83	45	100			P	P	P		N	P	0.68	I	D	P	5	9(5+4)
4	JAYASEELAN	60	42	100		P			N	N	N	N	0.76	I	D	P	4	7(3+4)
5	PALAYAM	76	68	19.7			P	P	P	P	N	P	0.54	I	D	P	5	8(5+3)
6	KANNAN	81	96	110			P	P	P	P	P	P	0.46	I	D	P	5	9(5+4)
7	KRISHNAMOORTHY	69	100	11.28			p	p	p	p	p	p	0.66	I	D	P	5	9(5+4)
8	MUNUSAMY	55	55	15.5			P	P	N	N	N	N	0.75	I	D	P	4	7(3+4)
9	SWAMINATHAN	65	45	65.5			P		N	N	N	N	0.86	I	D	P	3	6(3+3)
10	VENKATESAN	75	43	100			P	P	N	N	N	N	0.77	I	D	P	4	7(4+3)
11	SRINIVASAN	60	45.27	38			P		P	N	N	N	0.74	I	D	P	5	8(5+3)
12	KANNAN	74	30	100			P	P	N	N	N	N	0.62	I	D	P	5	9(5+4)
13	JAMAL	56	38	11	P				N	N	N	N	0.64	I	D	P	4	8(4+4)
14	APPADURAI	75	42	23	P				P	P	P	N	0.58	I	D	P	5	9(5+4)
15	RAMAMOORTHY	78	37	50			P		N	P	N	N	0.72	I	D	P	5	7(4+3)
16	SADAGOPPAN	69	61	100			P	P	N	N	N	P	0.71	I	D	P	5	7(4+3)
17	ETHIRAJ	72	38	8.31			P	P	P	P	P	N	0.77	I	D	P	4	7(3+4)
18	PALANI	67	90	20			P		P	P	P	P	0.62	I	D	P	5	9(5+4)
19	ANGAMUTHU	68	52	38			P	P	P	P	P	N	0.68	I	D	P	4	8(4+4)
20	MANIMARAN	78	52	100		P			N	P	N	P	0.71	I	D	P	5	8(4+4)
21	MOIDEEN	70	39	5.5			p	p	p	p	p	p	0.71	I	D	P	4	7(3+4)
22	KRISHNAMOORTHY	50	40	100			P		N	N	N	N	0.85	I	D	P	3	6(3+3)
23	KANAGARAJ	65	38	8	P				N	N	N	N	0.87	I	D	P	4	6(3+3)
24	GOVINDHAN	78	48	11		P			N	N	N	N	0.81	I	D	P	4	6(3+3)
25	RAMAN	59	32	20	P				N	N	N	N	0.87	I	D	P	4	6(3+3)

PZ-Peripheral Zone,CZ-central zone, TZ- Transition Zone, SVI- Seminal Vesicle Invasion,NVB-Neurovascularbundle involvement, ECE- Extra Capsular Extension, LN- Lymph Node,
DWI- Diffusion Weighted Imaging, ADC- Apparent Diffusion Coefficient, MRS- MR Spectroscopy, DCE- Dynamic Contrast Enhancement, P-Positive, N-Negative, I- Increased, D-Decreased
PI-RADS - Prostate Imaging Reporting & Data System

<u>ஆராய்ச்சி ஒப்புதல் கடிதம்</u>

ஆராய்ச்சி தலைப்பு

காந்த அதிர்வு அலை வரைவின் (எம்ஆர்ஐ) வேறு வரிசைகளைப்பயன்படுத்தி பெறப்படும் ஆண்மைச்சுரப்பி புற்று நோயின் முடிவுகளை கேளா ஒலி வரைவின் துணையோடு ஆசனவாய் வழியாக பெறப்படும் ஆண்மைச்சுரப்பி புற்றுநோய் திசு ஆய்வுச் சோதனை முடிவுகளுடன் ஒப்பிட்டு ஆய்வு செய்தல்

பெயர்	:	தேதி	:
வயது	:	உள் நோயாளி எண்	:
பால்	:	ஆராய்ச்சி சேர்க்கை எண்	:

இந்த ஆய்வு மூலம் திசு ஆய்வு சோதனைககு முன்னரே, ஆண்மைச்சுரப்பி புற்றுநோய் கட்டியின் தன்மையும் அதன் வீரியத்தையும் முன்கூட்டியே அறிய உதவும் என்பதை அறிவேன்.

இந்த ஆராய்ச்சியின் விவரங்களும் அதன் நோக்கங்களும் முழுமையாக எனக்கு தெளிவாக விளக்கப்பட்டது.

எனக்கு விளக்கப்பட்ட விஷயங்களை நான் புரிந்துகொண்டு எனது சம்மதத்தை தெரிவிக்கிறேன்.

இந்த ஆராய்ச்சியில் பிறரின் நிர்பந்தமின்றி என் சொந்த விருப்பத்தின்பேரில் பங்கு பெறுகின்றேன். இந்த ஆராய்ச்சியில் இருந்து நான் எந்நேரமும் பின்வாங்கலாம் என்பதையும் அதனால் எந்த பாதிப்பும் ஏற்படாது என்பதையும் நான் புரிந்துகொண்டேன்.

நான் இந்த ஆராய்ச்சியின் விபரங்களைக் கொண்ட ஆராய்ச்சித் தகவல் தாளைப் பெற்றுக் கொண்டேன்.

இதன் மூலம் எந்த பின்விளைவும் ஏற்படாது என்று மருத்துவர் மூலம் தெரிந்து கொண்டு, நான் என்னுடைய சுய நினைவுடனும் மற்றும் முழு சுதந்திரத்துடனும் இந்த மருத்துவ ஆராய்ச்சியில் என்னை சேர்த்துக்கொள்ள சம்மதம் தெரிவிக்கிறேன்.

தேதி: **பங்கேற்பாளர்–**

ஆராய்ச்சி தகவல் தாள்

காந்த அதிர்வு அலை வரைவின் (எம்ஆர்ஐ) பல்வேறு வரிசைகளைப்பயன்படுத்தி பெறப்படும் ஆண்மைச்சுரப்பி புற்று நோயின் முடிவுகளை கேளா ஒலி வரைவின் துணையோடு ஆசனவாய் வழியாக பெறப்படும் ஆண்மைச்சுரப்பி புற்றுநோய் திசு ஆய்வுச் சோதனை முடிவுகளுடன் ஒப்பிட்டு ஆய்வு செய்தல்

இந்த ஆய்வு மூலம் திசு ஆய்வு சோதனைககு முன்னரே, ஆண்மைச்சுரப்பி புற்றுநோய் கட்டியின் தன்மையும் அதன் வீரியத்தையும் முன்கூட்டியே அறிய உதவும் என்பதை தெரிவித்துக் கொள்கிறேன்.

இந்த ஆராய்ச்சியில் பங்கேற்பது தங்களுடைய விருப்பத்தின் பேரில் தான் இருக்கிறது. மேலும் நீங்கள் எந்நேரமும் இந்த ஆராய்ச்சியிலிருந்து பின்வாங்கலாம் என்பதையும் தெரிவித்துக் கொள்கிறோம்.

இந்த சிறப்பு சிகிச்சையின் முடிவுகளை ஆராய்ச்சியின்போது அல்லது ஆராய்ச்சியின் முடிவின் போது தங்களுக்கு அறிவிக்கப்படும் என்பதையும் தெரிவித்துக் கொள்கிறோம்.

ஆராய்ச்சியாளர் கையொப்பம் **பங்கேற்பாளர் கையொப்பம்**

நாள் :
இடம் :